

2019-01-01

Development Of An Iridium-Ceramic Substrate Catalyst Bed For The Decomposition Of Ionic Green Liquid Monopropellants

Alejandro Andre Vazquez
University of Texas at El Paso

Follow this and additional works at: https://digitalcommons.utep.edu/open_etd



Part of the [Mechanical Engineering Commons](#)

Recommended Citation

Vazquez, Alejandro Andre, "Development Of An Iridium-Ceramic Substrate Catalyst Bed For The Decomposition Of Ionic Green Liquid Monopropellants" (2019). *Open Access Theses & Dissertations*. 2907.

https://digitalcommons.utep.edu/open_etd/2907

This is brought to you for free and open access by ScholarWorks@UTEP. It has been accepted for inclusion in Open Access Theses & Dissertations by an authorized administrator of ScholarWorks@UTEP. For more information, please contact lweber@utep.edu.

DEVELOPMENT OF AN IRIIDIUM-CERAMIC SUBSTRATE CATALYST BED FOR THE
DECOMPOSITION OF IONIC GREEN LIQUID
MONOPROPELLANTS

ALEJANRO ANDRE VAZQUEZ

Doctoral Program in Mechanical Engineering

APPROVED:

Ahsan Choudhuri, Ph.D., Chair

Jack F. Chessa, Ph.D.

Joel Quintana, Ph.D

Luis Rene Contreras-Sapien, Ph.D.

Stephen L. Crites, Jr., Ph.D.
Dean of the Graduate School

Copyright ©

by

Alejandro A. Vazquez

2019

Dedication

This Dissertation is dedicated to my family and all their support, and my close friends that helped me through the hardest times.

DEVELOPMENT OF AN IRIIDIUM-CERAMIC SUBSTRATE CATALYST BED FOR THE
DECOMPOSITION OF IONIC GREEN LIQUID
MONOPROPELLANTS

by

ALEJANDRO ANDRE VAZQUEZ, MS, BS

DISSERTATION

Presented to the Faculty of the Graduate School of

The University of Texas at El Paso

in Partial Fulfillment

of the Requirements

for the Degree of

DOCTOR OF PHILOSOPHY

Department of Mechanical Engineering

THE UNIVERSITY OF TEXAS AT EL PASO

December 2019

Acknowledgements

I would like to give a great deal of gratitude to my family for supporting me and pushing me to reach as far as I can with my endeavors. I would like to thank Dr. Choudhuri for the opportunity to do this research and for the many hours of mentoring. I would like to acknowledge all my colleagues at the cSETR for their help in my research. A special recognition goes to Jaclyn Mejia, Raul Cuevas, and Jonathan Valenzuela. Without their help, many parts of this research would not have been completed in the time allowable. I would also like to thank Dr. Ahsan Choudhuri for his guidance and expertise.

WARNING This document contains technical data whose export is restricted by the Arms Export Control Act (Title 22, U.S.C., Sec 2751, et seq.) or the Export Administration Act of 1979 (Title 50, U.S.C., App. 2401 et seq.), as amended.

Violations of these export laws are subject to severe criminal penalties.

Disseminate in accordance with provisions of DoD Directive 5230.25.

Abstract

In an effort to advance green monopropellant propulsion using ionic liquids, the Center for Space Exploration and Technology Research (cSETR) has developed a pellet based catalyst bed for the decomposition of AF-M315E. The present paper will go over some of the fundamental research conducted towards the development of a catalyst bed and some of its applications. Three different catalyst bed designs were produced where each uses a different ceramic substrate material. The three different substrates are aluminum oxide, tungstated zirconia, silicon carbide each coated with iridium as the catalyst material. An experimental setup for testing the catalytic decomposition AF-M315E was built. The system utilizes a syringe pump as the propellant source flow the propellant through the catalyst be at specified flow rates. Current tests have shown decomposition temperatures up to 1400°C for flow rates in the range of 0.195 to 0.341 g/s for all three catalyst beds. The duty cycle conducted on these catalyst beds also revealed the silicon carbide based catalyst to perform the best in terms of lifetime.

Table of Contents

Acknowledgements.....	v
WARNING This document contains technical data whose export is restricted by the Arms Export Control Act (Title 22, U.S.C., Sec 2751, et seq.) or the Export Administration Act of 1979 (Title 50, U.S.C., App. 2401 et seq.), as amended. Violations of these export laws are subject to severe criminal penalties. Disseminate in accordance with provisions of DoD Directive 5230.25.	
Abstract.....	v
Table of Contents.....	vii
List of Tables.....	viii
List of Figures.....	ix
Chapter 1: Introduction.....	1
1.1 Cube Satellites Background.....	1
1.2 Project Overview.....	1
1.3 Monopropellant Systems.....	2
1.4 Project Objective.....	4
1.5 Practical Relevance.....	4
1.6 Literature Review.....	4
Chapter 2: Methodology.....	8
2.1 Catalyst Bed Description.....	8
2.2 Experimental Setup.....	8
2.3 Catalyst Holder.....	12
2.4 Data Acquisition.....	14
2.5 Electronic Configuration.....	16
2.6 Preliminary Testing.....	18
2.7 Catalyst Substrate Strength Reinforcement.....	24
2.8 Test Matrix.....	27
Chapter 3: Experimental Results.....	29
3.1 Catalytic Decomposition Temperatures of AF-M315E.....	29
3.2 Duty Cycle Testing of Catalyst Bed Substrates.....	32
3.3 Catalyst Bed Iridium Loss.....	41
Chapter 4: Summary and Conclusion.....	46
4.1 Summary.....	46
4.2 Conclusion.....	46
Chapter 5: Future Work.....	48
5.1 Lattice Pressure Drop Tests.....	48
References.....	51
Vita.....	52

List of Tables

Table 1: Instrumentation and Component List	18
Table 2: Test Matrix for Pellet Compression Tests	26
Table 3: Test Matrix for Duty Cycle Testing of the Three Different Catalyst Beds	28
Table 4: Percentage of Materials Present on Silicon Carbide Pellet Post Duty Cycle Testing	45
Table 5: Lattice Cube Pressure Drop Test Results	49
Table 6: Lattice Cube Sizes and Names	50

List of Figures

Figure 1: Orbital Factory X Propulsion Module.....	2
Figure 2: Busek Co. First Catalyst Bed Design [8]	5
Figure 3: Busek Co. Alternate Catalyst Bed Design [8].....	6
Figure 4: AF-M315 Catalytic Decomposition Experimental Setup Schematic.....	10
Figure 5: Experimental Setup for AF-M315E Catalytic Decomposition Studies.....	11
Figure 6: 1N Sea Level Nozzle Attachment	12
Figure 7: CAD Model of Catalyst Holder.....	13
Figure 8: Catalyst Holder Heating Profile with 6 Cartridge Heaters	14
Figure 9: Guide User Interface for Catalytic Decomposition Studies	15
Figure 10: NI LabVIEW Block Diagram for AF-M315E Catalytic Decomposition Studies.....	16
Figure 11: Electronic Setup for AF-M315E Catalytic Decomposition Studies.....	17
Figure 12: Thermal Decomposition of AF-M315E at 400°C Initial Temperature	19
Figure 13: AF-M315E Decomposition Temperatures with Alumina w/0% Loading Factor at 400°C Initial Temperature	20
Figure 14: AF-M315E Catalytic Decomposition using Alumina Catalyst Bed with 10% Iridium Loading Factor	21
Figure 15: Aluminum Oxide Catalyst Bed with 10% Iridium Loading Factor after First Decomposition Test	22
Figure 16: AF-M315E Catalytic Decomposition Temperatures using Alumina Catalyst Bed with 12% LF.....	22
Figure 17: AF-M315E Catalytic Decomposition Temperatures using Alumina Catalyst Bed with 14.8% LF.....	23
Figure 18: AF-M315E Catalytic Decomposition Temperatures using Tungstated Zirconia Catalyst Bed with 4.2% LF	24
Figure 19: Compression Test Machine with Single Iridium Coated Alumina Pellet	25
Figure 20: Stress-Strain Plot for Single Alumina Pellet Coated with 12% Iridium by Weight....	25
Figure 21: AF-M315E Catalytic Decomposition Temperatures with Aluminum Oxide Catalyst Bed (TC-101).....	30
Figure 22: AF-M315E Catalytic Decomposition Temperatures with Tungstated Zirconia Catalyst Bed (TC-101).....	31

Figure 23: AF-M315E Catalytic Decomposition Temperatures with Silicon Carbide Catalyst Bed (TC-102)	32
Figure 24: Aluminum Oxide Catalyst Bed Duty Cycle Experiments.....	33
Figure 25: Aluminum Oxide Catalyst Bed after Duty Cycle Testing. 22% of Pellets Fractured .	34
Figure 26: Aluminum Oxide Catalyst Bed Duty Cycle Averaged Temperatures for 0.24 g/s of AF-M315E	35
Figure 27: Tungstated Zirconia Catalyst Bed Duty Cycle Experiments.....	36
Figure 28: Tungstated Zirconia Catalyst Bed after Duty Cycle Testing. 100% of Pellets Fractured	37
Figure 29: Tungstated Zirconia Catalyst Bed Averaged Duty Cycle Temperatures for 0.24 g/s of AF-M315E	38
Figure 30: Silicon Carbide Catalyst Bed Duty Cycle Experiments	39
Figure 31: Silicon Carbide Catalyst Bed after Duty Cycle Testing with 0% of Pellets Fractured	40
Figure 32: Silicon Carbide Catalyst Bed Duty Cycle Averaged Peak Temperatures for 0.24 g/s of AF-M315E	41
Figure 33: Silicon Carbide Catalytic before Catalytic Decomposition Experiments	42
Figure 34: Scanning Electron Microscopy Analysis on Pellets near the Outlet Section	43
Figure 35: Scanning Electron Microscopy Analysis on Pellets near the Middle Section	43
Figure 36: Scanning Electron Microscopy Analysis on Pellets near the Inlet Section.....	44
Figure 37: Materials Present on a Silicon Carbide Pellet	45
Figure 38: Lattice Pressure Drop Test Experimental Setup.....	48
Figure 39: Lattice Pressure Drop Test Experimental Schematic	49

Chapter 1: Introduction

1.1 Cube Satellites Background

With the rise of the microsatellite, specifically the CubeSat or Cube Satellite, many universities in the United States have become more interested in space applications [1]. These CubeSats are typically used for low earth orbit and have rose in popularity in the new millennium because of their relatively low cost. They vary in size depending on the application but the most common dimension is a 10 by 10 by 10 cm chassis that incorporates all of its components and payload technologies within this volume [2]. Since CubeSats are already very limited in volume, monopropellant systems would be favorable bi-propellant systems due to simplicity in flight hardware. The monopropellant that has mostly been used in past decades is hydrazine. While offering the performance necessary in terms of specific impulse and thrust levels, hydrazine comes with many hazards. Therefore, the efforts of the past decade have been focused on alternative green monopropellants that can replace this hazardous hydrazine [2].

1.2 Project Overview

At the Center for Space Exploration and Technology Research at the University of Texas at El Paso, a CubeSat propulsion module is being developed. This propulsion module will be a part of a 2U CubeSat know as Orbital Factory X or OFX. OFX will have 3D printing capabilities, hence the name, and also have maneuvering capabilities with a monopropellant system. Specifically, the propulsion system will use four 1N monopropellant thrusters and six other micro cathode thrusters. The monopropellant used will be AF-M315E. The CAD model of the propulsion module with its components can be seen below if figure 1.

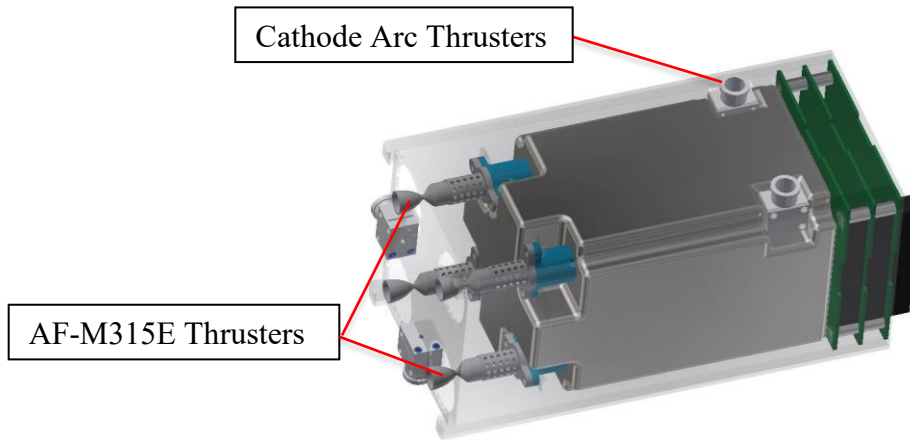


Figure 1: Orbital Factory X Propulsion Module

1.3 Monopropellant Systems

Monopropellant systems work on the principal of chemical decomposition of a single fluid. The fluid is required to be slightly unstable and release high amounts of heat energy when it decomposes. This high amount of heat energy creates the high temperatures inside of a thrust chamber that causes the acceleration and momentum exchange of particles. Decomposition of this chemical or monopropellant is caused by thermal energy, a catalyst, or both. Catalytic decomposition can occur at either room temperature or at elevated temperatures, depending on the type of monopropellant used.

As previously mentioned, hydrazine has been the dominant propellant when it comes to monopropellant systems. It has been an industry standard for several past decades, especially in the 20th century, because it provided the best performance in terms of specific impulse from other monopropellants. Hydrazine however is a very toxic and flammable chemical that poses numerous health hazards when handling and operating. Therefore, much of the effort in the propulsion community has been dedicated to finding a suitable alternative to hydrazine that can provide relatively the same performance without all the hazards. In recent years the Center for Space

Exploration and Technology Research has investigated the performance and characteristics of several of these safer monopropellants. The three propellants investigated by cSETR are High Test Peroxide, LMP-103s, and AF-M315E and these fall into the category of “Green Monopropellants”. The term green comes from the fact that the chemicals are more environmentally benign.

High test peroxide is a homogenous solution consisting of aqueous a mixture of hydrogen peroxide and water. Several different concentrations are used typical in the range of 86-98%, and cSETR has mostly focused on using 90% concentration. The theoretical decomposition products species of high test peroxide are oxygen and steam. It has been found that solid silver catalysts are the most effective when it comes to the propellant decomposition. HTP has a specific impulse in range of 150s [6].

LMP-103S is an ionic ammonia dinitramide (ADN) based liquid homogenous solution. The solution itself contains fuel/oxidizer mixture. This green monopropellant was developed in 1997 by the Ecological Advanced Propulsions Systems (ECAPS) in Sweden [7]. It is superior when compared to hydrazine in storability, handling safety, and performance with a specific impulse in the range of 252s.

AF-M315E is another ionic monopropellant that was created in and by the Air Force Research lab in 1998. Similar to LMP-103S, it contains a fuel/oxidizer mixture among other components. Specifically, AF-M315E is an aqueous homogenous solution consisting of hydroxyethylhydrazine nitrate (HEHN), hydroxylammonium nitrate, and water, and also ammonium nitrate (AN). It has both a higher density and a higher specific impulse when compared to hydrazine, resulting in an overall higher density-specific impulse of 50%. The ionic compounds in the solution keep it in liquid form due to their coulombic attraction. This greatly reduces the danger of toxic gases filling the container or the surrounding since essentially no AF-M315E

vapors are formed. Leakage of the propellant is also classified as critical, as opposed to hydrazine leakage classified as catastrophic, failure which would result in a simpler system with less components and overall mass [5].

1.4 Project Objective

The objective of this project is to develop a catalyst bed that is efficient in decomposing AF-M315E and can withstand the high temperatures of the reaction. This objective is tested in two sets of experiments. The first set of experiments is conducted to determine the temperatures that the catalytic decomposition of AF-M315E yields and therefore determine if effective decomposition is occurring. The second set of experiments is conducted to determine the catalyst bed lifetime by duty cycle testing.

1.5 Practical Relevance

The most widely used monopropellant for attitude control and reaction control systems is hydrazine. However, as previously mentioned, this monopropellant is extremely dangerous when handling and operating. The potential safer alternative that can replace hydrazine is AF-M315E which superior in virtually every way. The only drawback of AF-M315E is that it is not a propellant that will decompose at room temperature. The propellant is required to be preheated and then exposed to an effective catalyst before any reaction can occur. Currently there aren't many catalyst designs nor heating methods for ionic propellants. Therefore an effective catalyst bed and heating method is required which will be the focus of this dissertation.

1.6 Literature Review

When it comes to monopropellant systems, the catalyst bed is one of the most important components because it is essentially, in combination with the propellant, what will drive force. The catalyst will serve to reduce the activation energy of the incoming propellant in order to greatly

increase the decomposition rate. Since AF-M315E is relatively new, only being around for the past few decades, studies found in literature for catalyst beds and AF-M315E are very limited. In fact currently only a handful of companies have produced working catalysts and thruster systems that incorporate the ionic propellant.

One of the companies that has produced a working catalyst bed for the decomposition of AF-M315E is Busek. Busek developed several robust catalyst designs which can be found in the patent “Long Life Thruster”. One such design consists of elongate wires or tubes of catalytic material, shown below in figure 2, such as platinum or iridium. The wires or tubes are held together in a bundle by the use of a metallic ferrule. This catalyst bed composed of the bundle of tubes is integrated into a thruster by welding the ferrule to the combustion or decomposition chamber, as shown in figure 2. This specific design has a scalability that allows for it to be integrated into three different thruster designs with force outputs of 0.1, 0.5, and 5N for thruster named BGT-X1, BGT-X5, and BGT-5, respectively [8].

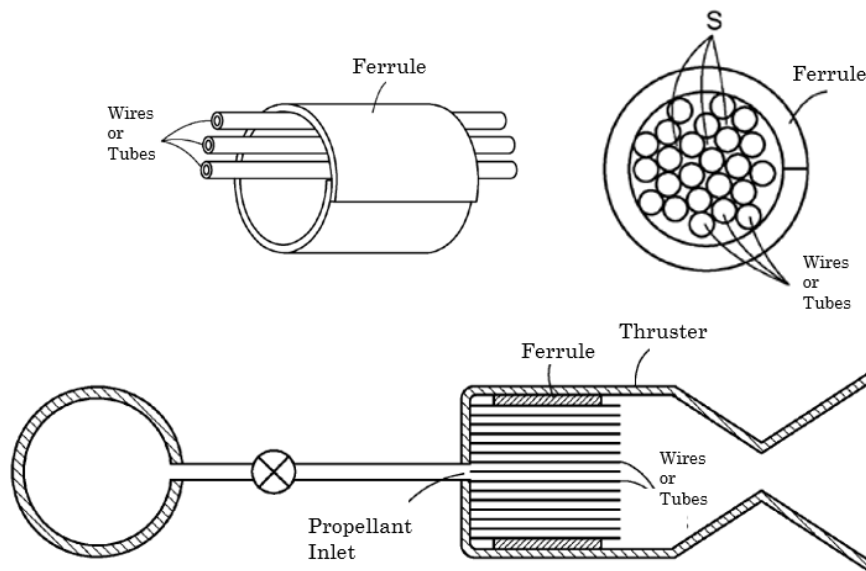


Figure 2: Busek Co. First Catalyst Bed Design [8]

Additionally, Busek developed an alternative catalyst reactor design found in the “Long Life Thruster” patent. The reactor design can be seen below in figure 3. It consists of two catalyst sections; a section containing iridium coated alumina pellets and a later section containing the bundled tubes of catalytic material as the previous design discussed prior. The first section with respect to the fluid flow, the iridium coated alumina pellets, is used primarily to evaporate and partially decompose the incoming AF-M315E. The propellant then follows into the second section of catalyst tubes where it fully decomposes. The alumina pellet section is kept relatively short to prevent exposing the ceramic pellets to the full decomposition temperatures of the AF-M315E and risk damaging the catalyst [8].

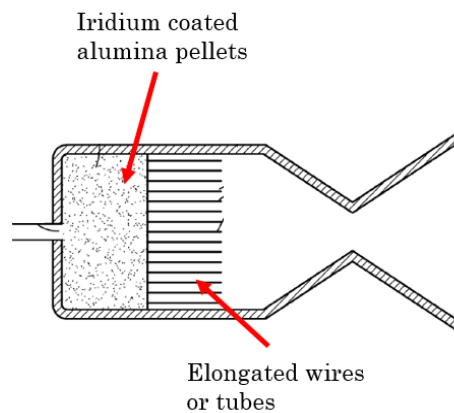


Figure 3: Busek Co. Alternate Catalyst Bed Design [8]

This iridium coated alumina pellet section is very similar to the catalyst design that is presented in this dissertation. The one major difference is that the catalyst bed that cSETR produced is able to withstand the full decomposition temperatures of the AF-M315E. A heat treatment method that significantly enhances the mechanical strength and therefore the lifetime of the catalyst bed was discovered and implemented. This heat treatment process and the strengthened catalyst bed pellets will be further discussed in later sections.

The NASA Space Technology Mission Directorate began an effort back in 2015 to develop a propulsion system module. This propulsion system was meant to be integrated into the payload of an ESPA-Launched Ball microsatellite. The system would use five of Aerojet Rocketdyne's GR-1 thrusters: 4 attitude control and 1 divert thruster. These GR-1 thrusters would use AF-M315E as the monopropellant and the patent pending catalyst bed design, LCH-240, from Aerojet Rocketdyne [5]. This LCH-240 catalyst design consists of 5% iridium on hafnium oxide granules. These granules range in size from 0.025 to 0.050 in [9]. The propulsion module and the GR-1 thruster can be seen below in figure 4. Although this project was never completed, the catalyst design used is very similar to the one presented in this dissertation, using small ceramic pieces coated in iridium.

Chapter 2: Methodology

2.1 Catalyst Bed Description

The catalyst beds used in this investigation are composed of stacked cylindrical ceramic pellets coated with iridium. Three different types of ceramics are used as the substrate material which results in three different catalyst beds. The first catalyst bed consists of aluminum oxide, or alumina, cylindrical pellets coated with 25% iridium loading factor by weight. The alumina pellets are on average 3 mm in both length and diameter. Approximately 100 of these coated pellets are stacked tightly in a cylindrical volume with a 0.385in diameter and a 1.5in length to make the first catalyst bed. The alumina ceramic is white in color.

The second catalyst bed consists of tungstated zirconia pellets coated with 25% iridium loading factor by weight. Tungstated zirconia were chosen over regular zirconia pellets in an attempt to reinforce the ceramic. These pellets are very similar in size to the alumina pellets, being 3mm in both length and diameter on average. Approximately 100 of these iridium coated tungstated zirconia pellets stacked in a volume of 0.385in diameter and a 1.5in length make up the second catalyst bed. The tungstated zirconia ceramic is white in color.

The third and final catalyst bed produced and tested consists of silicon carbide pellets coated with iridium. These pellets are also cylindrical in shape with average size of 1.5mm in both length and diameter. They are coated with an iridium loading factor of 25% by weight. Since these pellets are smaller in size, about 420 of these tightly stacked in the volume mentioned make up the third catalyst bed. The silicon carbide ceramic is black in color.

2.2 Experimental Setup

A test rig at cSETR was assembled to run the AF-M315 catalytic decomposition experiments. Figure 4 below shows the experimental schematic that is used with all of its components. The setup begins with a syringe pump that injects the propellant into the system at a

specified volumetric flow rate. A Genie Plus infusion pump is used for this. Most of the calculations done at cSETR are done using mass flow rate rather than volumetric flow rate so a conversion is made using the density of AF-M315E at room temperature, 1.46 g/cm. The fluid then flows through a series of hand operated and check valves before reaching the catalyst holder. The catalyst holder is piece that is used to contain the catalyst bed and preheat it to an initial temperature of 400°C. The catalyst bed needs to be preheated to 400°C before any decomposition can begin to occur. The catalyst holder part will be discussed in more detail in the next section. Decomposition temperature and pressure measurements are taken and recorded. The primary function of this experimental setup is to decompose the propellant and record the conditions inside the reaction chamber using temperature and pressure transducers. However, this test rig is also designed with the capabilities of capturing the decomposed species or gases of AF-M315E. This secondary function will come into play once the AF-M315E has decomposed and left the catalyst holder. Following downstream of the catalyst holder is another series of hand operated and solenoid valves before reaching the sample cylinders. The sample cylinders is where the decomposed gases are collected after closing the inlet valve. In order for gas to be collected without any outside contaminants, vacuum in the system is pulled prior to beginning experimentation. The vacuum is achieved by the use of a venturi device. The venturi device is connected perpendicular to the main line and high velocity gas is flown through it. The high velocity gas causes a pressure drop in the system by the venturi principle. Once the gage indicates the pressure is low enough, the isolation valve is shut to maintain the vacuum. The sample cylinders with the collected gases are then transferred to a mass spectrometer and subject to chemical composition analysis. An acrylic enclosure surrounds the catalyst holder to safely exhaust any potential leaks. A helium tank

is connected to the main line to purge the system of residual gases once testing has concluded for the day.

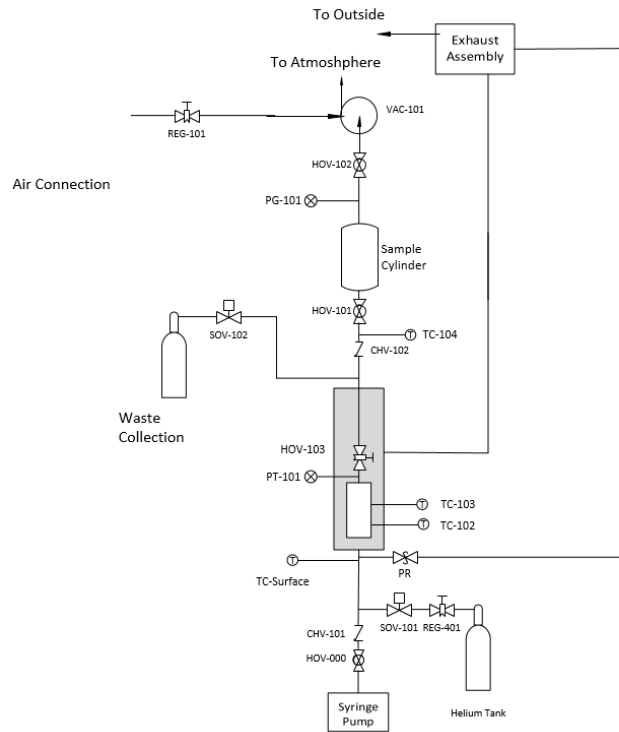


Figure 4: AF-M315 Catalytic Decomposition Experimental Setup Schematic

The experimental setup assembled with all of its components can be seen below in figure 5. The figure shows the exhaust system attached to the acrylic enclosure. Several different sample cylinders are attached in parallel. These sample cylinders range in size volume capacity from 300 to 1000 ml.

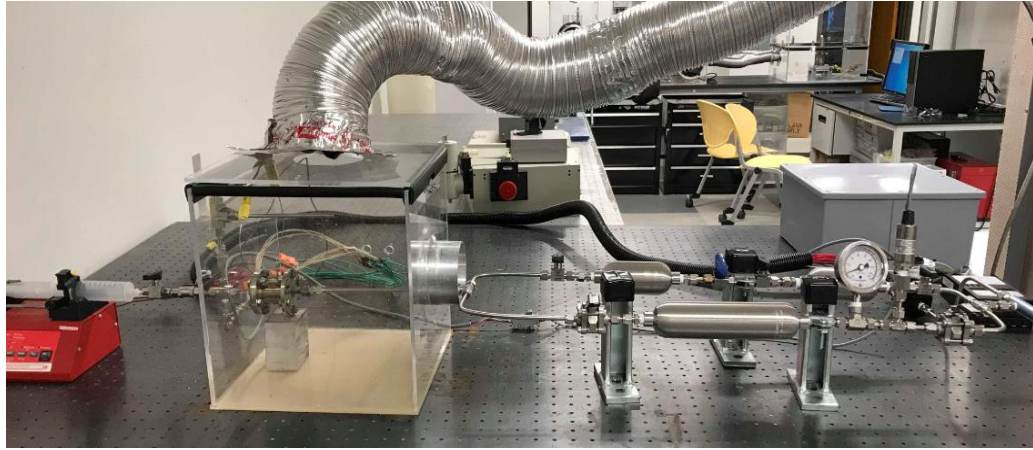


Figure 5: Experimental Setup for AF-M315E Catalytic Decomposition Studies

In order to obtain pressure measurements that can closely simulate those that would be created inside a 1N thruster, a thruster attachment was designed. It was designed with a nozzle expansion for El Paso ambient pressure and a thrust level of 1N. This thruster attachment connects directly to the outlet of the catalyst holder piece. This is accomplished by disconnecting HOV-103 in figure 4. This effectively disconnects the entire system downstream of HOV-103 and is then replaced by the thruster attachment piece. This thruster attachment piece is shown below in figure 6. The attachment, shown on the left of figure 6, has two ports on opposite ends of the combustion chamber. One of the ports is for temperature measurement and the other is for pressure measurement conditions inside of chamber during AF-M315E decomposition.



Figure 6: 1N Sea Level Nozzle Attachment

2.3 Catalyst Holder

The stacked pellets that compose the catalyst beds are held inside of a part called the catalyst holder. The inner cylindrical volume of this piece has dimensions of 0.385in for its diameter and 1.5in for its length. The catalyst holder has two major functions. The first function is to house the catalyst bed inside during catalytic decomposition experiments, as just mentioned. The second major function is the preheating of the catalyst bed to the initial desired temperature before beginning the experiments. The CAD model of the catalyst holder piece can be seen below in figure 7. The part was machined out of Inconel 718 in order to withstand the high decomposition temperatures of the exothermic reaction. In the figure, the yellow cylinder represents the placement of the catalyst bed. Six cartridge heaters are used to preheat the catalyst bed to the desired temperature of 400°C. The cartridge heaters each have an output of 100 watts. With a total of 600 watt output, it takes the system approximately 25 minutes to preheat the catalyst bed to 400°C. The cartridge heaters can be seen in figure 7 as red cylinders inserted around the perimeter of the catalyst bed. The part also has two Swagelok stem fittings attached to its outer surface. The fittings are used to attach K-type thermocouples. These thermocouples run all the way down to the center of the holder, where they measure the direct decomposition temperature of the AF-M315E. The

first thermocouple, denoted either TC-01 or TC-101, is located at the point 25% of the catalyst bed length. The second thermocouple, denoted either TC-02 or TC-102, is located at the point 50% or halfway the length of the catalyst bed. Silver plated stainless steel O-rings are used to seal the inlet and outlet interfaces of the catalyst holder.

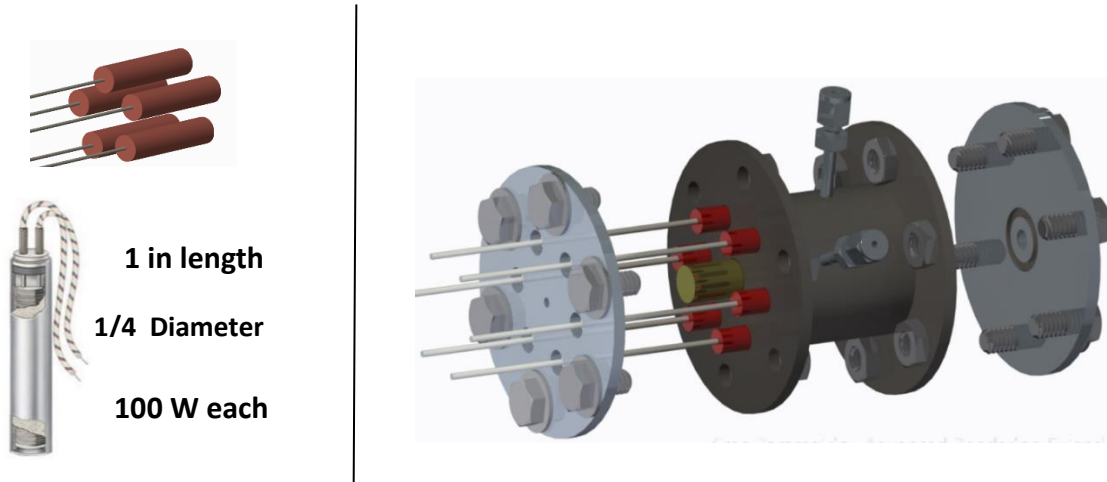


Figure 7: CAD Model of Catalyst Holder

The heating profile for the catalyst bed using the six cartridge heaters is shown below in figure 8. Starting at room temperature the catalyst bed begins rising rapidly in temperature then slows down as it gets closer to the goal temperature. It takes a total of about 1500s or 25 minutes to rise to 400°C.

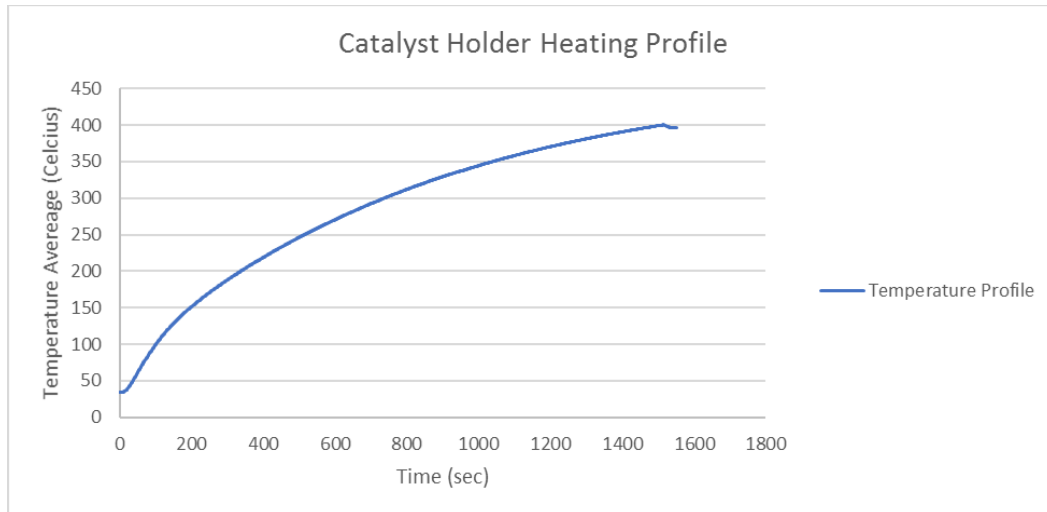


Figure 8: Catalyst Holder Heating Profile with 6 Cartridge Heaters

2.4 Data Acquisition

The catalyst decomposition studies are conducted using NI LabVIEW program. Figure 9 below shows the user interface with the toggle switches for the purge and drain valves. An LED indicator signals when the system heaters have been activated. TC-102 and TC-103 are the temperature data reading for the thermocouples situated directly on the catalyst bed. The Labview VI uses the temperature reading of TC-102 to control the heaters. Once TC-102 reaches 400°C, the heaters are turned off and turned back on if the system falls below the said temperature. TC-surface measures the temperature of the catalyst holder outer wall and TC-104 measures the temperature inside the thruster attachment directly downstream of the catalyst bed. A pressure gage indicator measures the voltage of the pressure transducer. The pressure transducer is located on the thruster attachment and takes readings of the conditions inside. The block diagram for the LabVIEW interface is shown in figure 10.

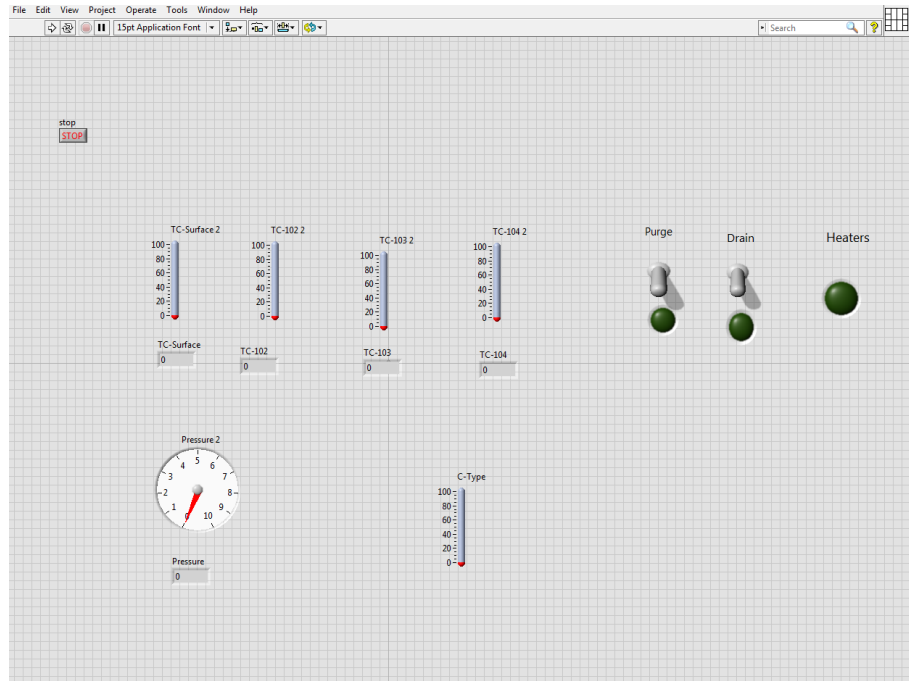


Figure 9: Guide User Interface for Catalytic Decomposition Studies

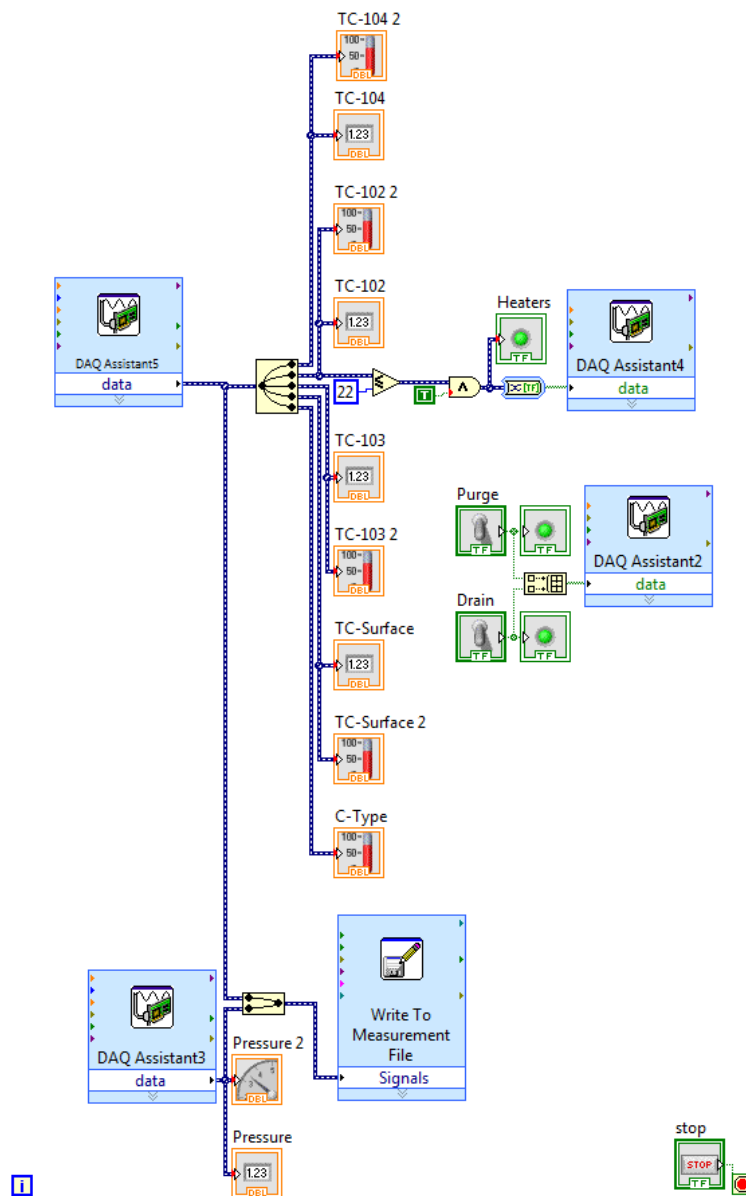


Figure 10: NI LabVIEW Block Diagram for AF-M315E Catalytic Decomposition Studies

2.5 Electronic Configuration

The electronic bus box containing all the electronic components is shown in figure 11. DAQ NI 9211 is used to acquire all the analog input signals for the thermocouples used in the system. DAQ NI 6008 is used to acquire the analog input signals from the pressure transducer and also to send the output digital signal to the relays. Three solid state AC relays are used to control the valves and the heaters in the setup. Relays labeled 101 and 102 are used to control the purge

valve and drain valve, respectively. The relay labeled 104 is used to control all six cartridge heaters. DAQ 6008 sends the voltage to the relays to activate them and allow the AC current to follow to the respective device. Table 1 below describes the physical connections as they are hooked up to the DAQs.

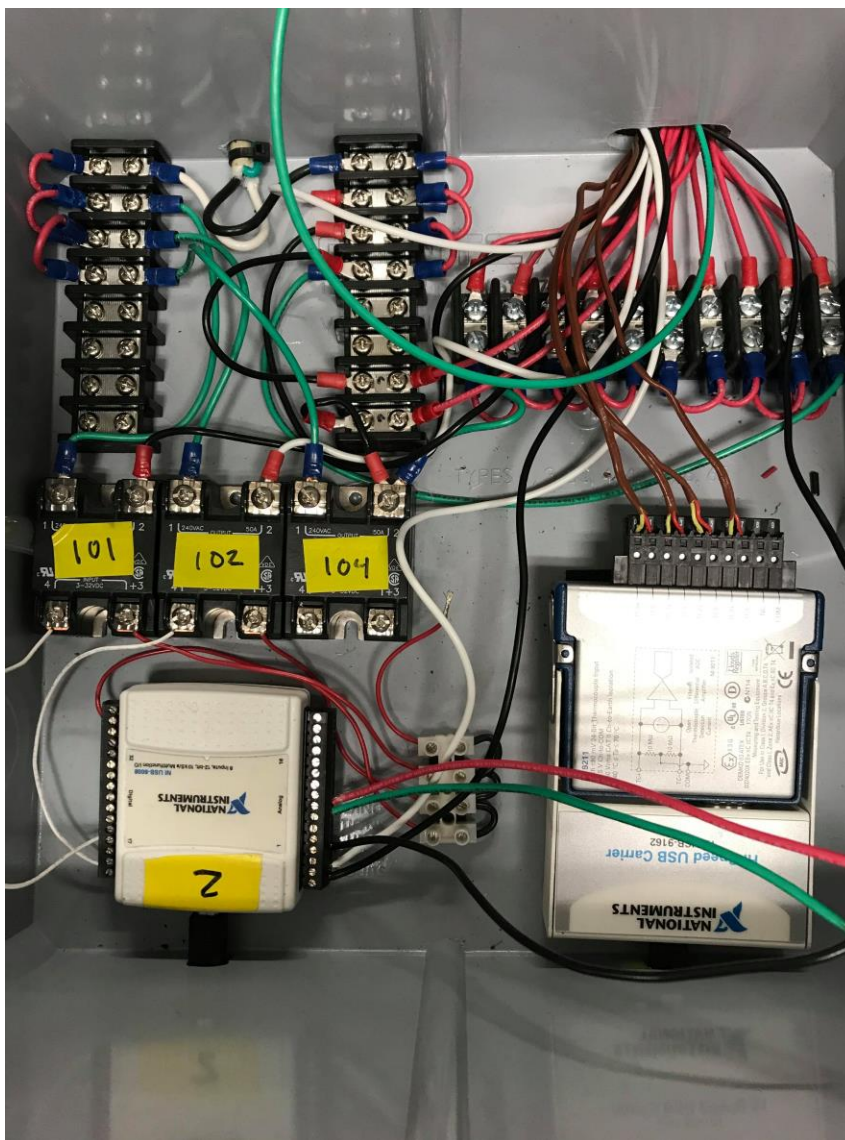


Figure 11: Electronic Setup for AF-M315E Catalytic Decomposition Studies

Table 1: Instrumentation and Component List

Component Identifier	Description	Data Acquisition and Device Number	Physical Channel Port Number	Signal Conditioner	Required Voltage
SP-1	Syringe Pump ac	N/A	N/A	N/A	120V ac
TC-Surface	Thermocouple	NI 9211	6 and 7	N/A	Provided by Thermocouple Hub (NI 9211)
TC-101	Thermocouple	NI 9211	0 and 1	N/A	Provided by Thermocouple Hub (NI 9211)
TC-102	Thermocouple	NI 9211	2 and 3	N/A	Provided by Thermocouple Hub (NI 9211)
TC-104	Thermocouple	NI 9211	4 and 5	N/A	Provided by Thermocouple Hub (NI 9211)
SOV-101	Solenoid Valve	Heaters (NI 6008)	17 and 32	N/A	120V ac
SOV-102	Solenoid Valve	Heaters (NI 6008)	18 32	N/A	120V ac
HEATERS	Cartridge Heaters	Heaters (NI 6008)	31 and 32	N/A	120V ac
PT-101	Pressure Transducer	Heaters (NI 6008)	20 and 32	SG-1	120 ac
PR	Pressure Relief Valve	N/A	N/A	N/A	N/A

2.6 Preliminary Testing

At the start of the project, the plan was to impregnate or coat alumina pellets and run experiments to investigate their effectiveness in decomposing AF-M315E. As a benchmark for quantifying the performance of the catalyst bed, the experimental system is first run with no

catalyst bed present. With no catalyst present the catalyst holder is preheated to 400°C and AF-M315E is flown through it at various flow rates. Figure 12 below shows the temperatures achieved with only thermal decomposition of the propellant. Both thermocouples showed a similar temperature profile, peaking close to the 700°C mark for TC-01.

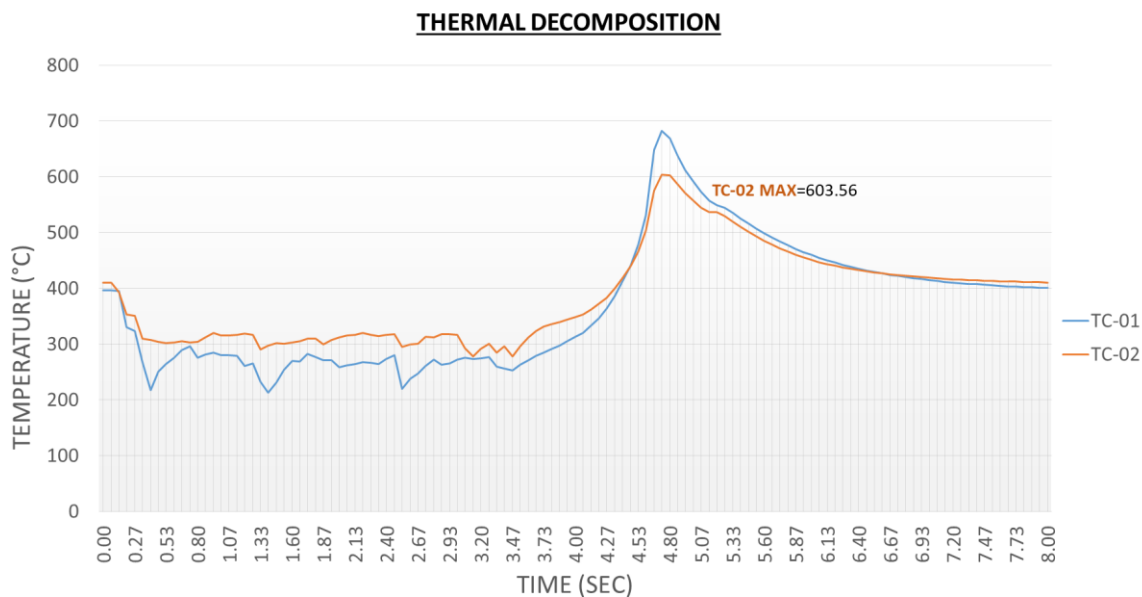


Figure 12: Thermal Decomposition of AF-M315E at 400°C Initial Temperature

After the thermal decomposition test of AF-M315E, a test using alumina pellets with no iridium coating was conducted using similar AF-M315E flow rates. Figure 13 below shows the decomposition temperature obtained using alumina pellets with a 0% iridium loading factor. This test was conducted to observe the changes in temperatures that occur between testing with nothing inside the catalyst holder (thermal decomposition) and testing with uncoated alumina pellets. As expected, the presence of the alumina pellets with no catalytic material coating caused the temperatures to peak to lower values since the pellets acted as a large thermal sink. The decomposition temperatures obtained reached values close the 600°C mark.

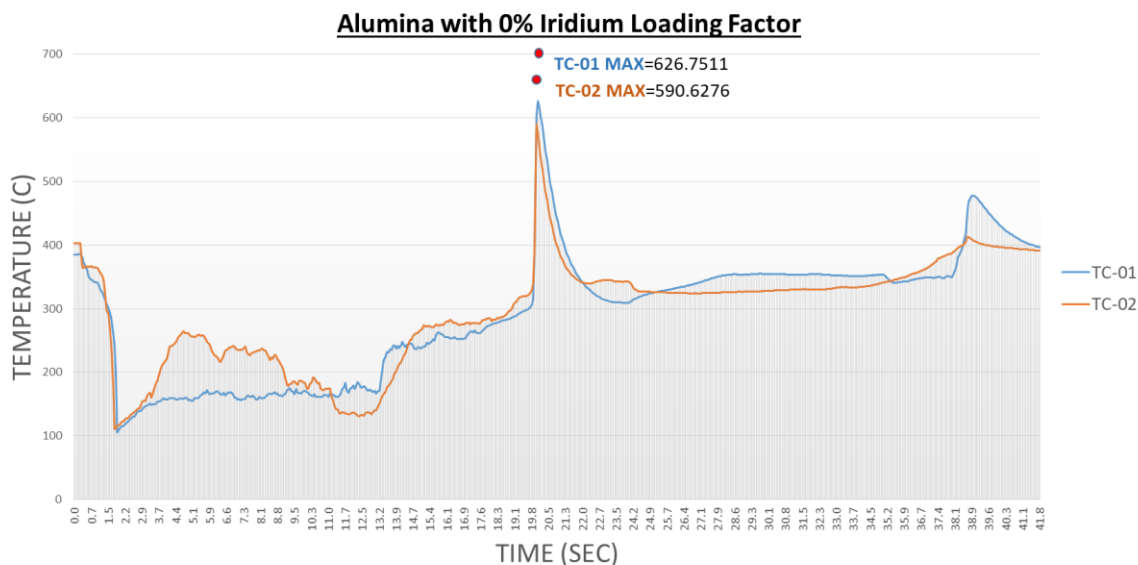


Figure 13: AF-M315E Decomposition Temperatures with Alumina w/0% Loading Factor at 400°C Initial Temperature

When the first series of tests were conducted with the iridium catalyst bed loaded, very strange catalyst bed temperature plots were recorded. The testing began as planned, at the initial catalyst preheated temperature of 400°C. Once the system reached 400°C, the syringe pump began injecting the AF-M315E into the system and through the catalyst bed. Figure 14 below shows this said erratic behavior captured by both thermocouples. At the start of the test, the quick drop in temperature is due to the evaporation of the water in the solution. In both temperatures readings, there is a sudden rise immediately after the water has evaporated, then the temperature continues to increase at a much slower rate before plummeting down and rising back up again. The catalyst bed was inspected after the test and it was noticed that the pellets had undergone structural damage. A portion of the pellets had fractured, exposing much of the aluminum oxide. A picture of the fractured pellets can be seen in figure 15. At first it was believed that the crumbling of the catalyst bed was what caused the multiple peaks and drops in temperature. As the pellets were broken down, the exposed alumina effectively reduced the surface area of the catalytic material. However,

as the catalyst bed continued to be broken down it approached its powder form, which is theoretically its most efficient form in terms of surface area. Therefore, there is a continuous toggle between the exposed alumina and the continuously decreasing particle size.

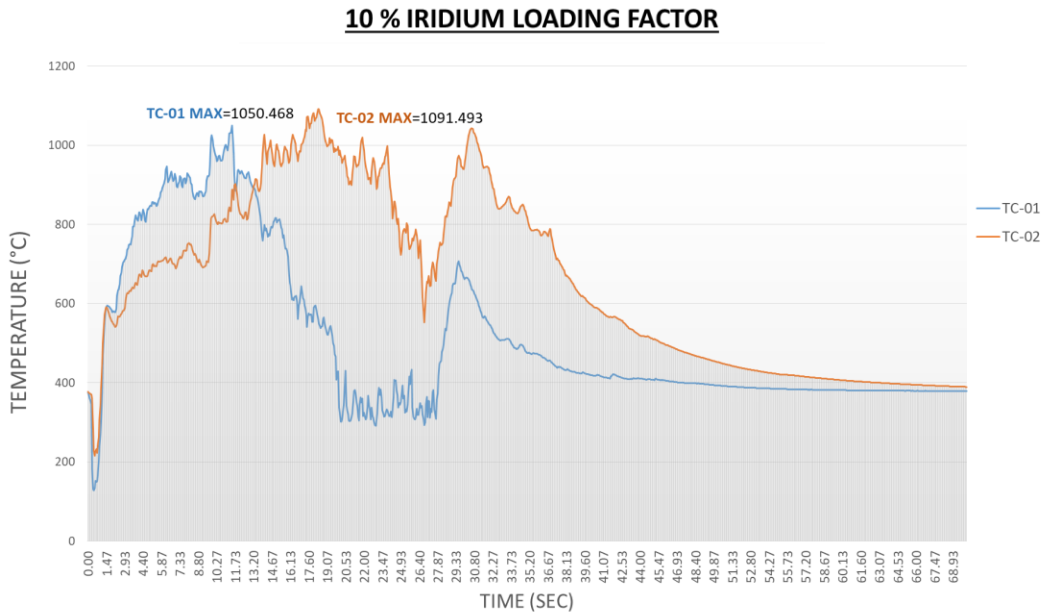


Figure 14: AF-M315E Catalytic Decomposition using Alumina Catalyst Bed with 10% Iridium Loading Factor

Figure 15 shows part of the aluminum oxide catalyst bed that was used in the first catalytic decomposition test. As can be seen, some of the pellets are still intact in its initial cylindrical form but many others were shattered into smaller irregular forms. This trend continued for every test thereafter using the same catalyst bed, rapidly reducing the pellets down to near powder form after only a handful of tests.

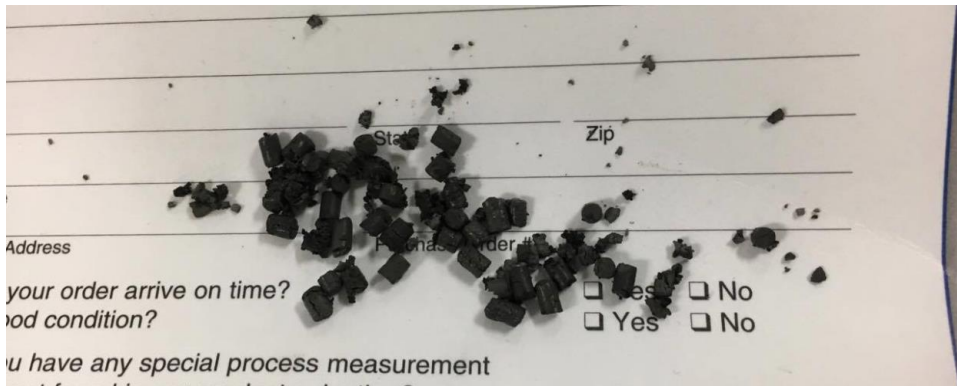


Figure 15: Aluminum Oxide Catalyst Bed with 10% Iridium Loading Factor after First Decomposition Test

The other batches of coated alumina pellets had an iridium loading factor of 12% and 14.8% by weight. Figures 16 and 17 below show two of the tests done for each respective iridium loading factor test. As expected, the higher iridium LF (Loading Factor) yielded higher temperatures. However, the catalyst beds continued to fail structurally.

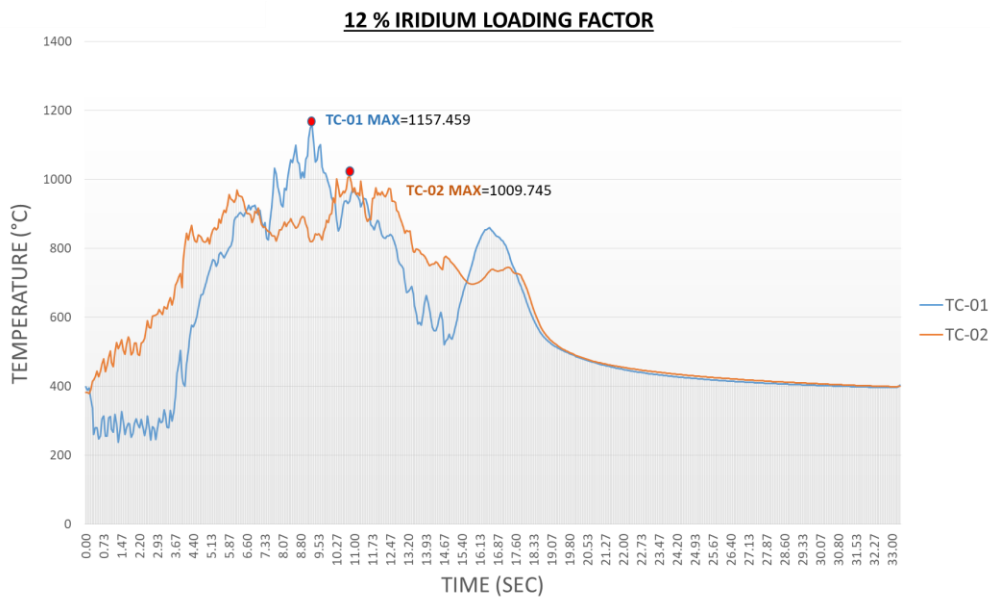


Figure 16: AF-M315E Catalytic Decomposition Temperatures using Alumina Catalyst Bed with 12% LF

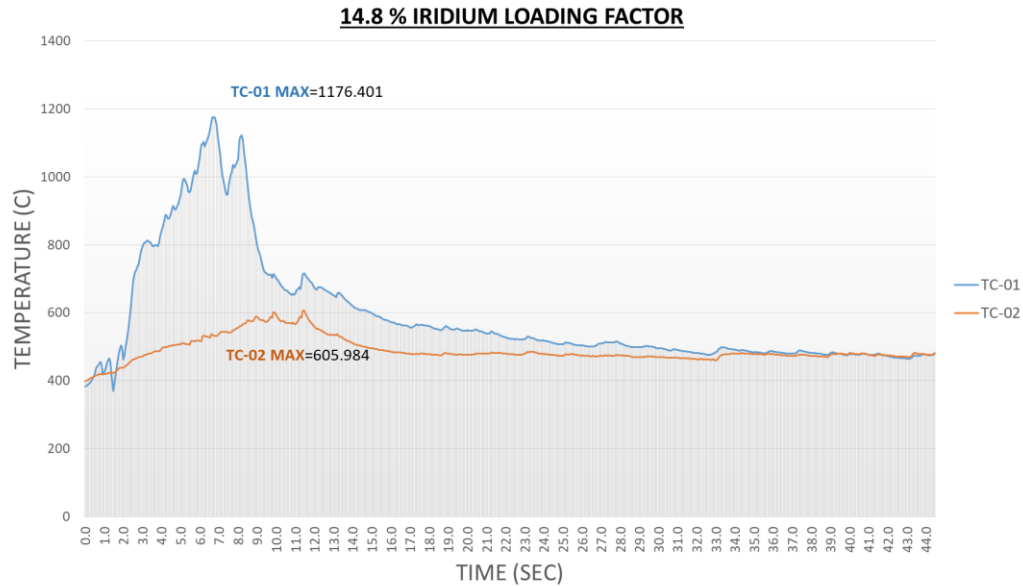


Figure 17: AF-M315E Catalytic Decomposition Temperatures using Alumina Catalyst Bed with 14.8% LF

A catalyst batch using tungstated zirconia coated with 4.2% iridium was also produced initially and tested. Figure 18 below shows the temperatures obtained with this batch. It is evident the temperatures were not nearly as high as the ones obtained using the alumina catalyst, with temperatures peaking only to the 800-900°C mark. This can be expected since the catalytic material was not as high. However, the tungstated zirconia catalyst bed had almost completely pulverized after one single test. It had pulverized significantly more than the alumina catalyst bed even though only one single test was conducted with this batch.

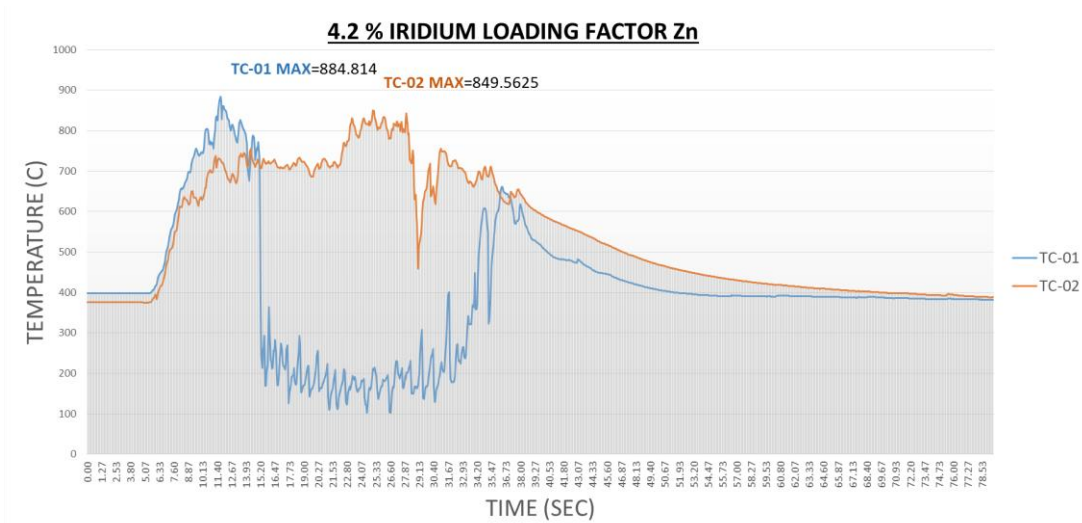


Figure 18: AF-M315E Catalytic Decomposition Temperatures using Tungstated Zirconia Catalyst Bed with 4.2% LF

2.7 Catalyst Substrate Strength Reinforcement

After the initial decomposition tests, shown in the previous preliminary testing section, were completed, it was hypothesized that the crumbling of the ceramic pellets was causing the unsteady temperatures. Although relatively high peak temperatures were achieved, the catalyst bed simply would not survive more than a few tests. This would render them impractical for spaceflight and propulsion systems since a new catalyst bed would need to be replaced frequently. Even if the catalyst bed was easily replaceable, the unsteady temperatures would create unsteady and unpredictable forces. Therefore it was imperative to reinforce the structural integrity of these catalyst beds.

One theory that was formulated involved the iridium loading factor of the catalyst beds. An inverse correlation was observed with between the iridium LF and the percentage of catalyst bed fracture. Therefore, it was hypothesized that increasing the loading factor of the catalytic material on the pellets would enhance their mechanical properties. This theory was tested by performing a series of compression tests on iridium coated alumina pellets. The small single pellet is seen placed on the compression machine in figure 19.



Figure 19: Compression Test Machine with Single Iridium Coated Alumina Pellet

The stress-strain plot in figure 20 was obtained using a pellet with iridium loading factor of 12%. It is evident that the pellet deforms in an elastic manner for the beginning of the compression test until about 8 MPa. After this point, the ceramic begins to experience plastic deformation for the remainder of the test until complete fracture is achieved. The orange sloped line is the trend line approximation for the young's modulus or modulus of elasticity.

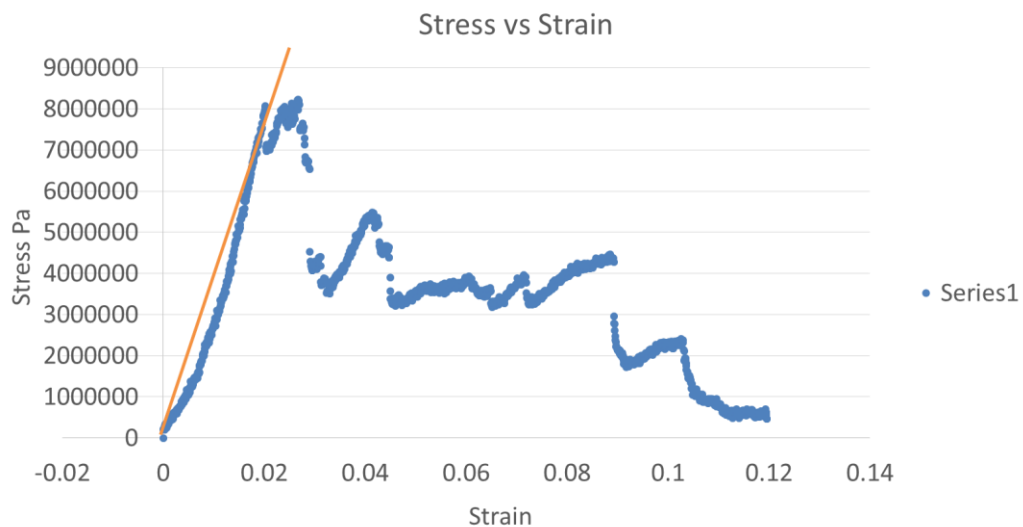


Figure 20: Stress-Strain Plot for Single Alumina Pellet Coated with 12% Iridium by Weight

Similar plots were obtained for the other different iridium loading factors tested. These tests can be seen in table 2 below. The table shows the modulus of elasticity obtained from each of the different loading factors tested. Some of the loading factors were tested multiple times to obtain a standard deviation. Another value that is found on this table is the modulus of resilience which is a measure of the material's toughness to resist fracture. The modulus of resilience is the value the team used for evaluating and comparing the mechanical strength of the coated ceramic. The modulus of resilience is calculated by obtaining the area under the stress-strain curve of each plot. Since the plots are not regular functions, a trapezoidal rule is implemented to numerical integrate and obtain the approximate area. The data, however, showed no reasonable correlation between loading factors as was hypothesized. Since the mechanical strength of the ceramic was not significantly affected by the iridium coating loading factor, an alternative approach was taken.

Table 2: Test Matrix for Pellet Compression Tests

Test	Loading Factor	Ur (Mpa)	E (Mpa)
3	0%	0.13438	285.5
4	11%	0.04705	174.9
5	12%	0.093404	452.1
6	14%	0.336868	161.4
7	20%	0.091902	420.8
8	0%	0.234134	165.7
9	0%	0.075742	360
10	0%	0.151374	374.1
11	11%	0.124556	194.4
12	11%	0.065709	339.8
13	11%	0.044546	245.9
14	12%	0.405712	129.2
15	12%	0.086078	639.3
16	12%	0.08357	338.7

After a team meeting with several subject matter experts, the Center for space Exploration and Technology Research decided to heat treat the ceramic pellets. Once the heat treatment process was complete, the pellets were tested one time to evaluate them. The decomposition temperatures

were higher and significantly steadier than before. The catalyst holder was opened and the pellets were inspected to reveal virtually no damage. It was then concluded that the heat treatment process successfully enhanced the mechanical strength of these ceramic pellets. The specific heat treatment process cannot be discussed in detail for proprietary reasons.

2.8 Test Matrix

With the new heat treated pellets, a test matrix was developed to test and evaluate the catalytic decomposition temperatures of AF-M315E using these catalyst beds. This test matrix is shown in table 2. The data will be useful when designing an Af-M315E thruster system because the temperatures in the combustion chamber will be similar. A separate test matrix was also developed for evaluating the lifetime of the catalyst beds. This test matrix, shown in table 3, involves a type of duty cycle testing. In this duty cycle tests the catalyst beds are first preheated to 400°C and then exposed to 30 seconds of AF-M315E decomposition. After the 30 seconds, the system is allowed to cool back down to 400°C before running propellant again through the catalyst bed for another 30 seconds. This cycle is repeated until the catalyst failure criteria is satisfied. In this case, the failure criteria is satisfied when the decomposition temperatures in the catalyst holder chamber fall below 1000°C. 1000°C was chosen because it is the temperature typically found with hydrazine systems. Therefore, if AF-M315E is producing temperatures equal or below those of hydrazine then its performance is no longer valuable to the propulsion system.

Table 3: Test Matrix for Duty Cycle Testing of the Three Different Catalyst Beds

Test Number	Catalyst Substrate	Flowrate (g/s)
1	1	0.049
2	1	0.097
3	1	0.146
4	1	0.195
5	1	0.243
6	1	0.292
7	1	0.341
8	2	0.049
9	2	0.097
10	2	0.146
11	2	0.195
12	2	0.243

Catalyst Substrate 1 = Alumina

Catalyst Substrate 2 = Zirconia

Catalyst Substrate 3 = Silicon Carbide

Chapter 3: Experimental Results

3.1 Catalytic Decomposition Temperatures of AF-M315E

The first set of experiments were conducted to determine the temperatures produced when the AF-M315E catalytically decomposes which each different catalyst bed. Several different flow propellants were chosen to obtain a range of decomposition temperatures. These propellant flow rates fall in the range of 0.05 to 0.341 g/s. The first catalyst bed tested was the alumina based, followed by the tungstated zirconia based, followed by the silicon carbide.

3.3.1 Aluminum Oxide Catalyst Bed

The aluminum oxide based catalyst bed consists of approximately 100 alumina pellets coated with iridium. The iridium coating for each pellet was 25% loading factor by weight. At first sight, the decomposition temperatures obtained are much steadier than the preliminary testing results. As before, the system was first preheated 400°C before running any AF-M315E through the catalyst. From figure 21 shown below, it can be seen that the temperatures begin to rise rapidly when the testing has commenced. After the first peak, the temperatures plateau and remain steady around an average value. This continues until the flow of propellant is stopped and the temperature plummets back down to the initial temperature. The flow rates were allowed to run for a minimum of 2 minutes to allow the system to reach steady state. The initial rise becomes steeper with increasing propellant flow rate, indicating a higher temperature gradient. However, at the higher flow rates, this difference in slope becomes much more insignificant. The highest temperatures achieved lie in the 1400°C mark. Also at the higher flow rates, 0.195 g/s and above, the temperatures begin to overlap or steady out around the same peak value. From this data it is deduced that increasing the AF-M315E flow rate past this point will not result in higher

decomposition temperatures for the current catalyst configuration. A temperature of 1400°C for the combustion chamber gases is enough to support a thrust of 1N in a monopropellant system.

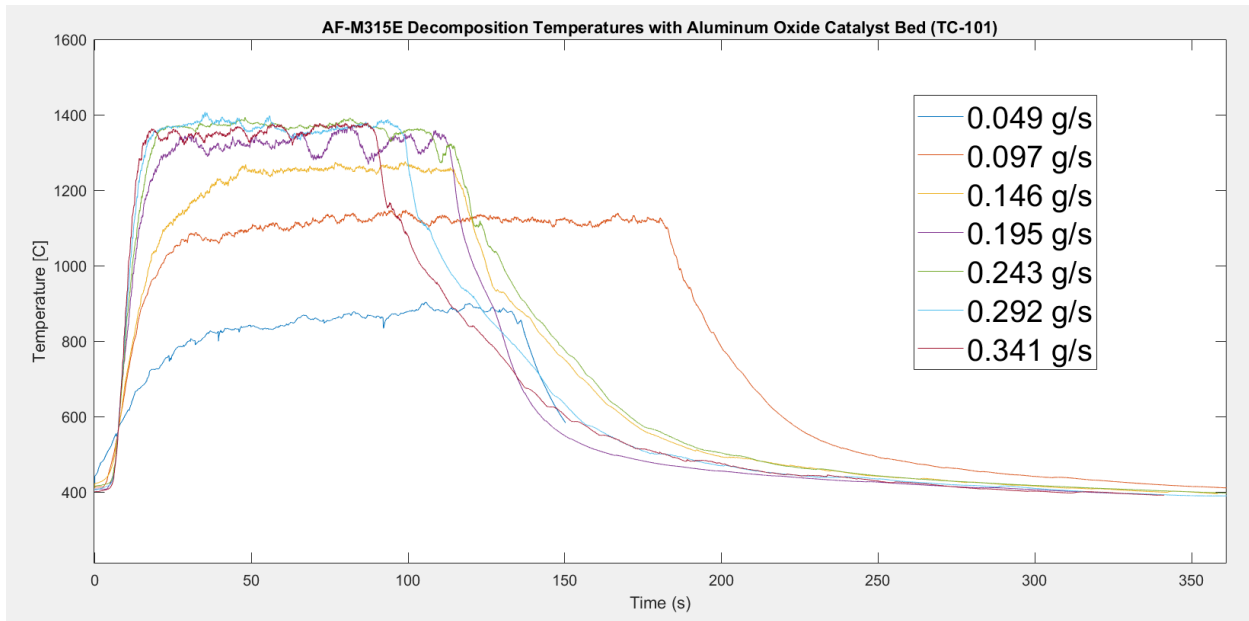


Figure 21: AF-M315E Catalytic Decomposition Temperatures with Aluminum Oxide Catalyst Bed (TC-101)

3.3.2 Tungstated Zirconia Catalyst Bed

The tungstated zirconia catalyst bed consists of approximately 100 tungstated zirconia pellets coated with iridium. The AF-M315E decomposition temperature plots obtained are very similar to those obtained using the alumina catalyst bed. This can be expected since both catalyst beds use the same coating of catalytic material, namely iridium. The tests begin at the preheated temperature of 400°C and rapidly rose to the peak temperatures where they plateaued and steadied out for the duration of the test. These plots are shown below in figure 22. The higher range of flow rates, specifically from 0.195 to 0.341 g/s of AF-M315E, produced temperatures very close to the 1400°C mark. As mentioned with the alumina catalyst bed, these 1400°C temperatures are enough to support thrust in a 1N AF-M315E thruster.

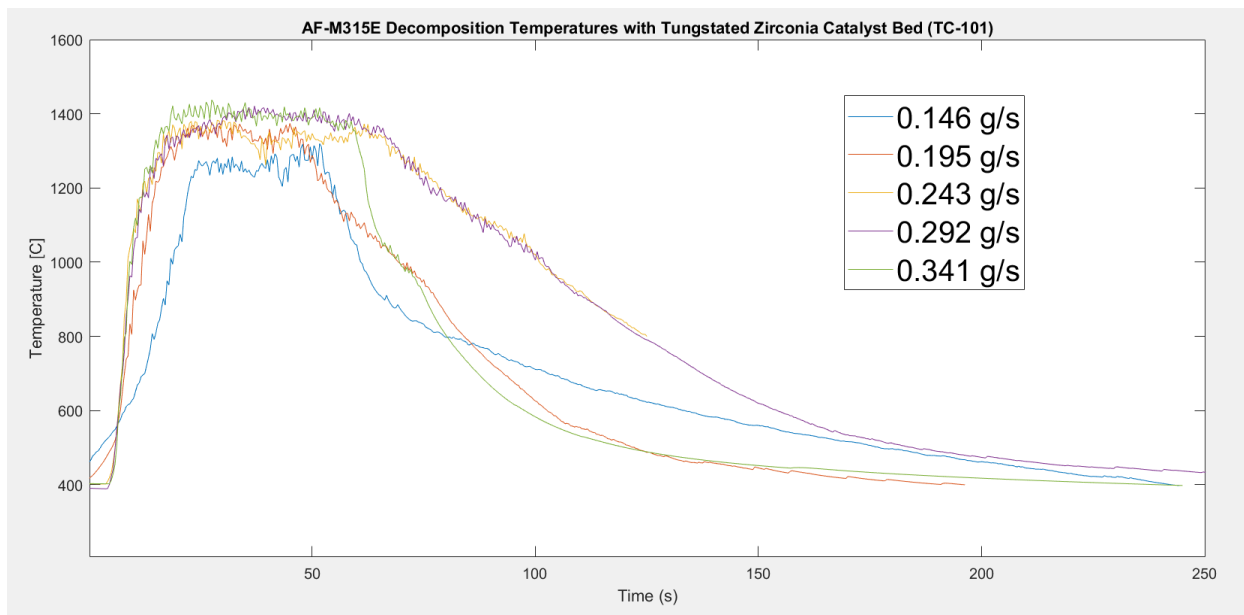


Figure 22: AF-M315E Catalytic Decomposition Temperatures with Tungstated Zirconia Catalyst Bed (TC-101)

3.3.3 Silicon Carbide Catalyst Bed

The last set of AF-M315E catalytic decomposition temperatures are shown below in figure 16. These temperatures were produced using the silicon carbide based catalyst bed. This catalyst bed consists of approximately 420 silicon carbide pellets coated with iridium. The iridium loading factor used is 25% by weight. One significant difference about these results from the previous two is the point of measurement. The temperatures shown in figure 23 were recorded with thermocouple TC-102, at the point half way of the catalyst bed length. The previous two results, figures 21 and 22, were obtained using TC-101. In the silicon carbide tests, TC-102 was used because technical difficulties caused the thermocouple at TC-101 port to fail. However, as mentioned in previous sections, it was observed that the temperature difference between TC-101 and TC-102 is almost always 200°, with TC-101 being the higher reading. With this information, and from figure 23, it is deduced that temperatures obtained at the TC-101 point are approximately in the same range for those obtained in figure 21 and 22. Therefore, the catalytic decomposition

temperatures produced by the silicon carbide catalyst bed are comparable to those obtained with the previous two catalyst beds. Once again, this was expected since the catalytic material is the same for all three catalyst beds. Fewer AF-M315E flow rates values chosen for testing because it was predicted that the lower values would yield relatively low temperatures.

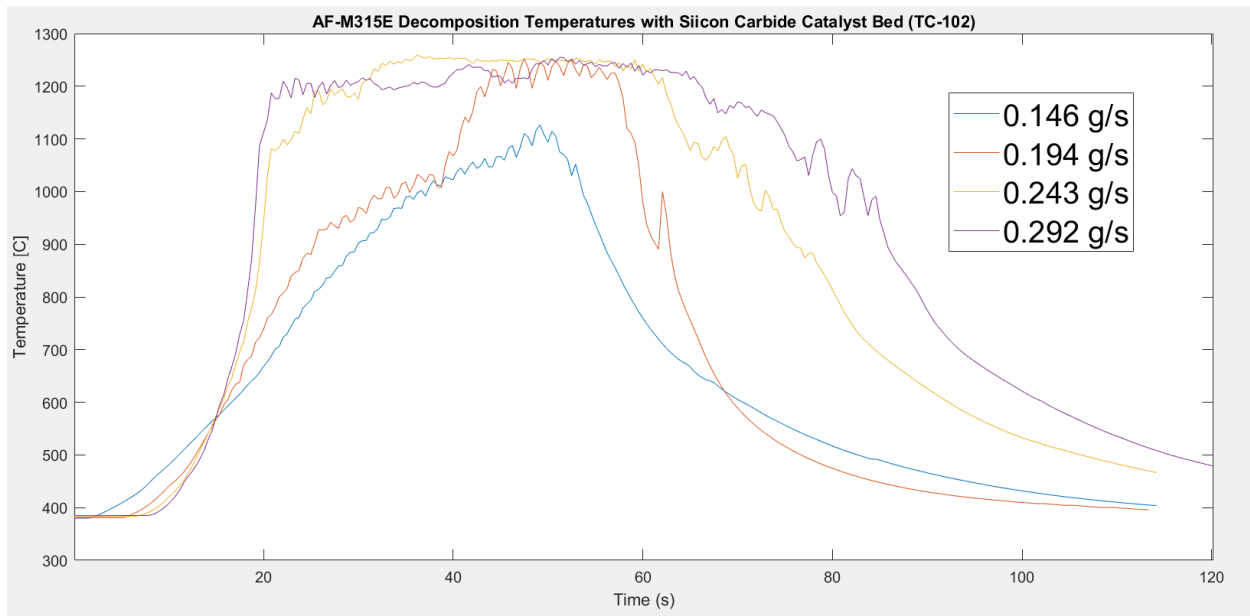


Figure 23: AF-M315E Catalytic Decomposition Temperatures with Silicon Carbide Catalyst Bed (TC-102)

3.2 Duty Cycle Testing of Catalyst Bed Substrates

3.3.1 Aluminum Oxide Catalyst Bed Duty Cycle

The entirety of the aluminum oxide catalyst bed duty cycle experiments are shown in one graph in figure 24. These are a total of 104 plots. As mentioned before, the duty cycle testing consists of exposing the catalyst bed to the Af-M315E decomposition temperatures for a specified flow rate for 30 second intervals. The flow rate chosen was 0.243 g/s because figures 21, 22, and 23 showed that flow rates above this value did not significantly increase the decomposition temperature of the catalyst bed. This would allow the system to reach the high temperatures without requiring too much propellant. As before with the decomposition tests, the duty cycle tests

begin at the initial catalyst bed temperature of 400°C. From figure 24, it can be seen that initially the decomposition temperatures reach the 1400°C. As the tests continue the plots begin to gradually drop in peak temperatures. In theory, this trend of decreasing decomposition temperature will continue until the peak temperature is approximately 700°C, the temperature produced when there is no catalyst bed is present in the system. However, once the decomposition temperatures reached approximately 1000°C, the duty cycle testing was considered complete and the catalyst holder was opened to inspect the pellets. The 1000°C mark was taken as the cutoff criteria because this is the temperature hydrazine produces when catalytically decomposed. If the system is allowed to produce temperatures below 1000°C, then in theory, it will perform worse than hydrazine.

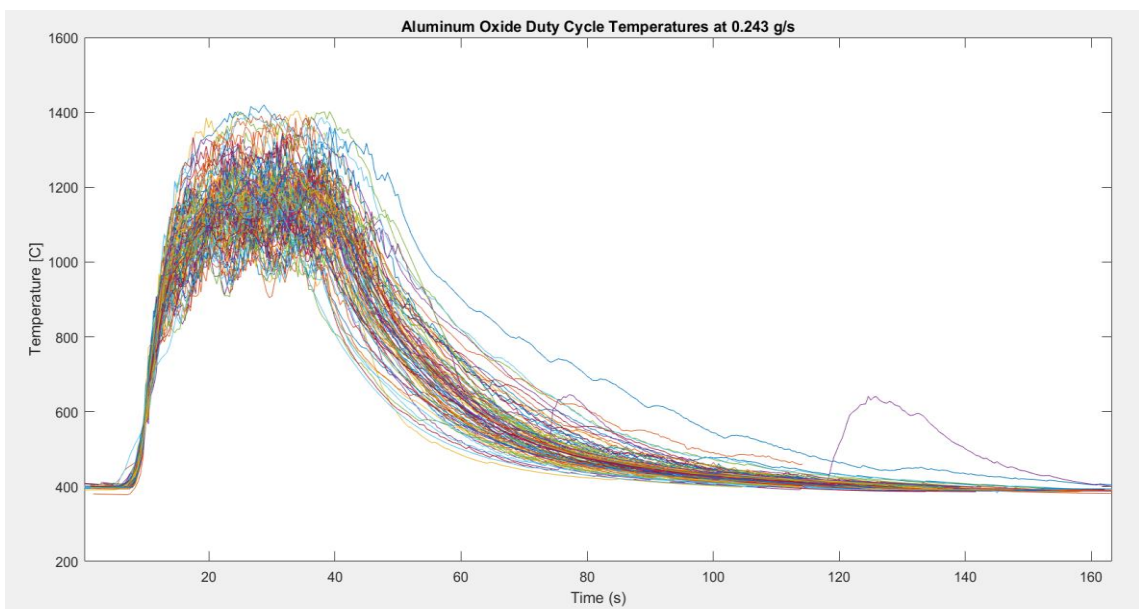


Figure 24: Aluminum Oxide Catalyst Bed Duty Cycle Experiments

Figure 25 below shows the aluminum oxide catalyst bed after the duty cycle was completed. In the figure 25, the pellets isolated to the left of the container are those which suffered damage in the form of fracturing and shattering. The rest of the pellets which suffered virtually no visible damage are on the right of the container. The percentage of pellets that fractured is approximately 22%. The total accumulated run time of 4203 s or 1.17 hr.



Figure 25: Aluminum Oxide Catalyst Bed after Duty Cycle Testing. 22% of Pellets Fractured

In figure 24, if all the temperature peaks are averaged out about the mean peak point, then the barcode of average temperatures, shown in figure 26, is obtained. From these average temperatures in figure 26, an average rate of decay can be calculated. The average rate of decay for the aluminum oxide catalyst bed is $13.46^{\circ}\text{C}/\text{Test}$. This means that the peak temperatures obtain from AF-M315E decomposition using the alumina catalyst bed is dropping by approximately 13 degrees Celsius every test. The 1N thruster that has been designed by the OFX team has a catalyst chamber that is identical to catalyst chamber inside the catalyst holder. The thruster is also being tested in firing periods of 30 seconds. Since the flow rates for both systems are relatively similar, it can be assumed that the conditions inside the 1N thruster will drop 13°C after every hot fire test. This will inadvertently also affect the thruster performance.

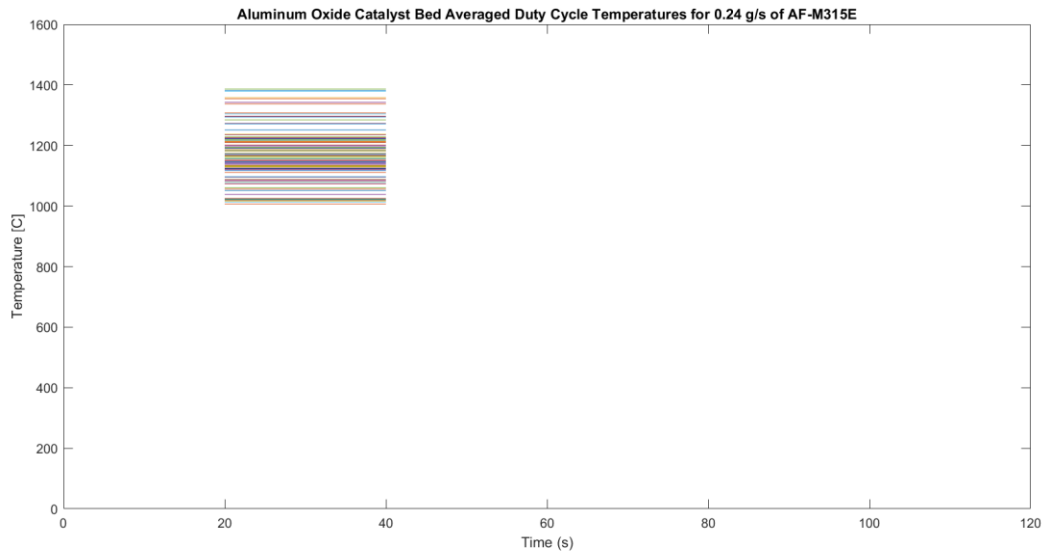


Figure 26: Aluminum Oxide Catalyst Bed Duty Cycle Averaged Temperatures for 0.24 g/s of AF-M315E

3.3.2 Tungstated Zirconia Catalyst Bed Duty Cycle

The tungstated zirconia duty cycle is also shown completely in one graph, figure 26. For these experiments, only 22 complete tests were conducted. On the 23rd test, thermocouple TC-101 began reading very strange temperature drops and peaks. These sudden drops and peaks resembled those obtained from the preliminary testing experiments. For this reason, it was assumed that the catalyst bed had suffered some damage and the duty cycle testing was ended. All twenty two decomposition temperature plots can be seen in figure 27. The temperature plots follow a similar trend to those from the aluminum oxide catalyst duty cycle tests. Initially the temperatures peak to the 1400°C mark and then gradually decay as the tests continue. Once again, the cutoff criteria was 1000°C for reasons explained in section 3.3.1. However, as seen from figure 27, the catalyst bed failed before the temperatures decayed down to 1000°C.

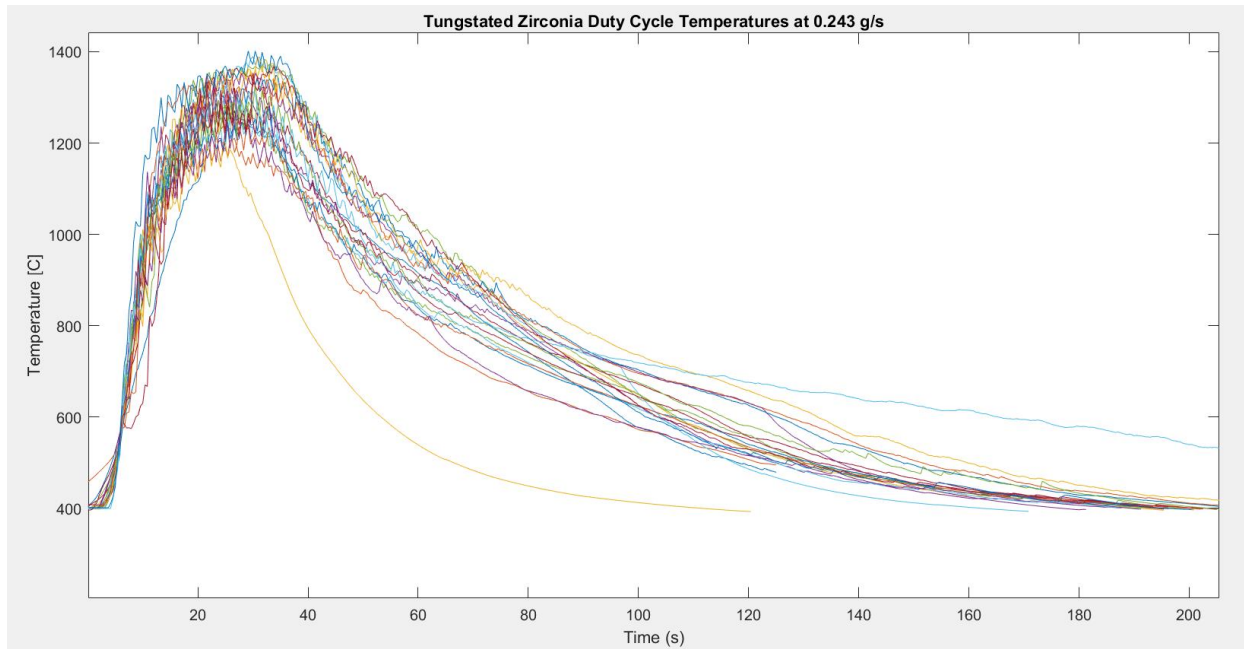


Figure 27: Tungstated Zirconia Catalyst Bed Duty Cycle Experiments

Once the duty cycle for the tungstated zirconia catalyst was completed, the catalyst holder was opened and the pellets were inspected. Figure 28 below shows the state of the catalyst bed after the duty cycle of 22 runs were completed. As seen, the pellets had completely fractured down to powder form with a few shards of ceramic. Although the most efficient configuration of a catalyst bed is powered form, it is not very practical for a simple monopropellant system. Without a sophisticated containment mechanism, the powder would quickly wash away in only a few thruster hot firings. For this reason, it is concluded that the tungstated zirconia catalyst bed performed significantly worse than the alumina catalyst bed in terms of lifetime. The total run time for this duty cycle experiment was 943 seconds or 15.7 minutes.



Figure 28: Tungstated Zirconia Catalyst Bed after Duty Cycle Testing. 100% of Pellets Fractured

Once again, the peak temperatures for the zirconia duty cycle were averaged about the mean point. This generated the temperature barcode shown in figure 29. From this, the tungstated zirconia was calculated to have a performance rate of decay of $15.05^{\circ}\text{C}/\text{Test}$. This means the temperature peaks inside of the catalyst holder were approximately 15°C lower for each successive test run.

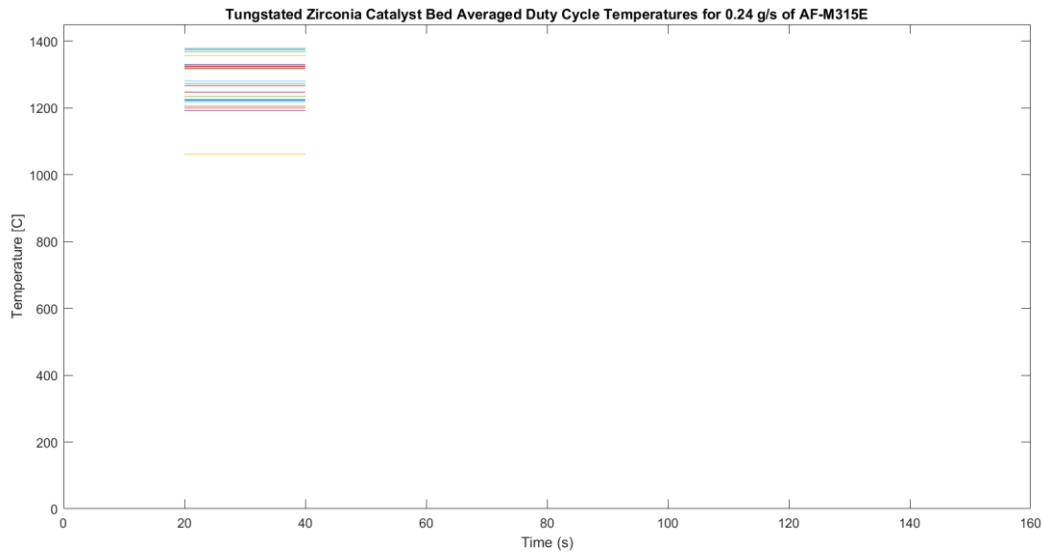


Figure 29: Tungstated Zirconia Catalyst Bed Averaged Duty Cycle Temperatures for 0.24 g/s of AF-M315E

3.3.3 Silicon Carbide Catalyst Bed Duty Cycle

The silicon carbide based catalyst bed duty cycle experiments can be seen in figure 30. The figure shows the graph containing all 101 duty cycle tests conducted using this catalyst bed. In a strikingly similar pattern to the duty cycle of tests of aluminum oxide, the silicon carbide temperatures rapidly rise and peak to their steady values. The values reach the 1400°C mark for the initial tests, then begin to gradually decay in peak temperature. Following the same failure criteria as the previous two duty cycle tests, the silicon carbide duty cycle was ended once the temperature began reaching levels of 1000°C. The duty cycle test lasted for 3680 seconds. The catalyst holder was opened to inspect the ceramic pellets for damage. Surprisingly enough, virtually no damage of the catalyst bed was visible present.

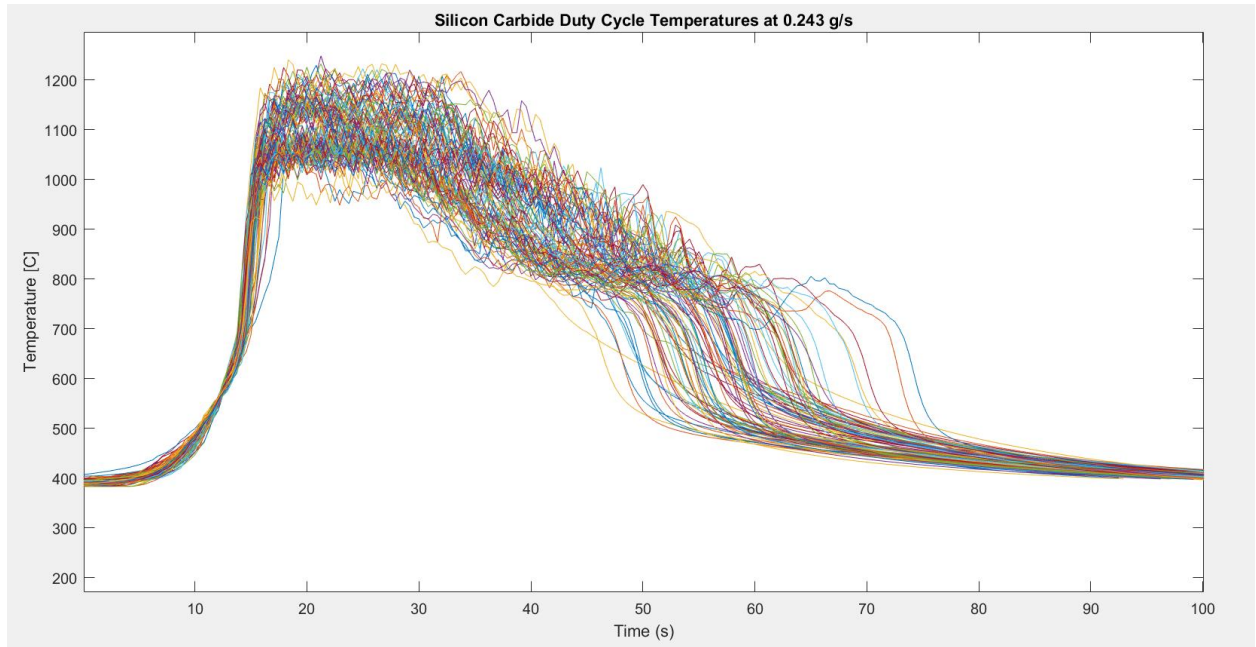


Figure 30: Silicon Carbide Catalyst Bed Duty Cycle Experiments

After the silicon carbide catalyst bed duty cycle was completed, the catalyst holder was opened to inspect the ceramic pellets for damage. Surprisingly enough, virtually no damage of the catalyst bed was visible present. The only irregularity found was a chunk of catalyst bed composed from several pellets bonded together presumably from the residual propellant. The catalyst bed after the duty cycle can be seen in figure 31 below. The results obtained from these set of experiments are interesting because the catalyst bed suffered practically no mechanical damage. In past tests it had been concluded that the decay in peak temperatures was due to the fracturing of the pellets. However, since the silicon carbide catalyst bed suffered no mechanical damage during the duty cycle testing, the same conclusion could not be drawn. One possible theory that the OFX team proposed is the washing away of the catalytic material from pellets. In other words, the flow of the liquid AF-M315E through the catalyst bed is gradually removing the iridium from the pellets after each test run. Since silicon carbide itself is black, same color as the iridium, it is difficult to visually observe any difference in color shading that would indicate loss of catalytic material.

Therefore, the post duty cycle pellets were subject to energy dispersive x-ray spectroscopy or EDS analysis. This EDS analysis will be discussed in more detail in later sections.



Figure 31: Silicon Carbide Catalyst Bed after Duty Cycle Testing with 0% of Pellets Fractured

If the temperature peaks in figure 30 are averaged, the remaining graph is a barcode of mean temperatures shown in figure 32. From these average temperatures, it can be calculated that silicon carbide catalyst bed performance rate of decay is $2.56^{\circ}\text{C}/\text{Test}$. This performance rate of decay is significantly smaller when compared to the rate of decay of the other two catalyst beds. This can be explained the significant difference in pellet fracture percentage between the catalyst beds. Since silicon carbide suffered virtually no fracture damage, it was able to maintain a more constant temperature peak throughout the duty cycle experiments.

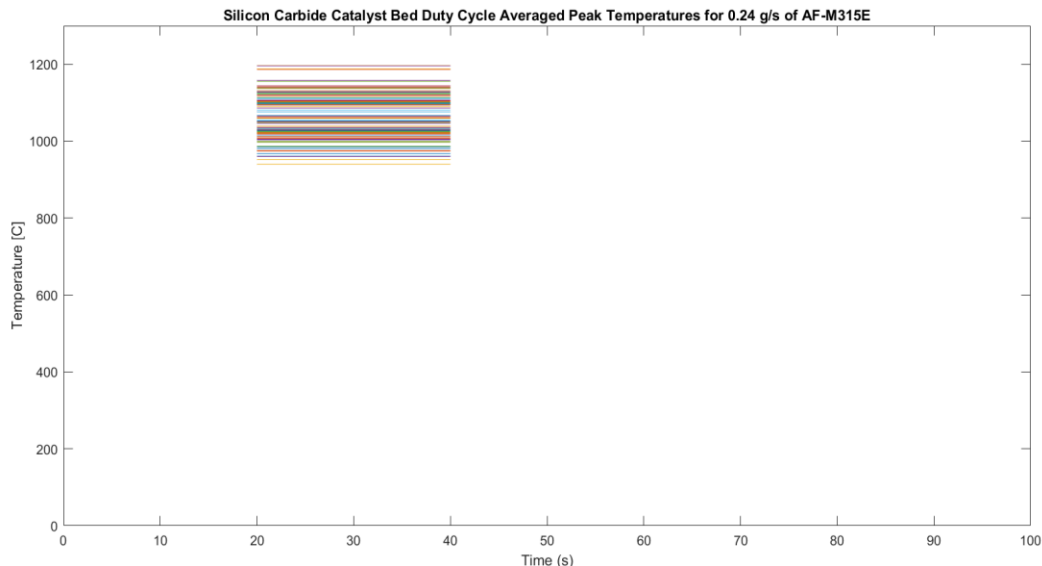


Figure 32: Silicon Carbide Catalyst Bed Duty Cycle Averaged Peak Temperatures for 0.24 g/s of AF-M315E

3.3 Catalyst Bed Iridium Loss

3.3.1 Silicon Carbide Catalyst Bed Chemical Microanalysis

With the virtually nonexistent fracture damage to the silicon carbide catalyst bed after the duty cycle testing, it was questioned as to why the system experienced a temperature decay. Since it was previously concluded that the cause of the temperature peaks decay was due to the fracturing of the pellets, there had to be something else responsible for this loss in AF-M315E decomposition performance with the silicon carbide pellets. One potential hypothesis was that the catalytic material, or iridium, was washing away from the pellets with each passing duty cycle test. As the pellets loose the iridium, the catalytic surface area of the catalyst bed is reduced, resulting in a loss of decomposition effectiveness. In order to test this hypothesis, a few silicon carbide catalyst pellets were subject to chemical microanalysis.

3.3.2 Scanning Electron Microscopy Analysis on Silicon Carbide Catalyst Bed

The scanning electron microscopy and energy dispersive x-ray spectroscopy analysis were performed on the silicon carbide catalyst bed to determine the amount of catalytic material that

had been lost during testing. The photos in figure 33 were taken before beginning the duty cycle experiments. The photos magnified 10 and 50 micro meters show how the catalytic material, or iridium, in white is distributed over a single silicon carbide pellet.

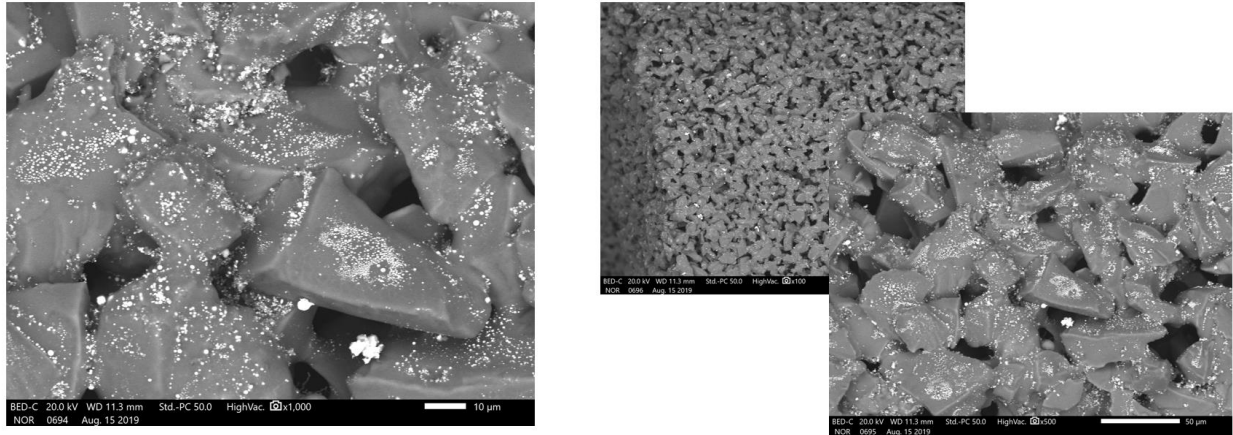


Figure 33: Silicon Carbide Catalytic before Catalytic Decomposition Experiments

After the duty cycle tests experiments were performed, three different set of photographs from the energy dispersive x-ray spectroscopy were taken. These three sets include photos taken for pellets near the inlet section, pellets near the middle section, and pellets near the nozzle attachment section. The reason for this division of three separate sections analysis is based on observations made during the AF-M315E catalytic decomposition tests. As discussed in earlier sections, it was mostly found that the decomposition temperatures were higher near the inlet of the chamber as indicated by the thermocouples TC-101 and TC-102. In fact, TC-101 would read approximately 200°C higher than TC-102. Therefore, it was hypothesized that the pellets would suffer the most mechanical damage near the inlet, followed by the middle, and lastly near the outlet. This hypothesis would also apply to the theory that the liquid propellant would wash away the catalytic material from the pellets. Near the inlet section, the pellets would be exposed to the most of the liquid phase propellant since the AF-M315E would not fully decompose until reaching the middle or end section of the catalyst bed. Therefore, the inlet section of the catalyst bed would

experience the most iridium loss, followed by the middle section, and lastly the section near the thruster nozzle attachment. Figure 34 shows three different magnification scales, 500 100 and 10 micro meters. From these figures, 34 to 36, we can see the amount of iridium present is virtually the same in the three sample pellets taken from each section. The darker spots on the images to right of the figures are spots of higher depth in the pellet.

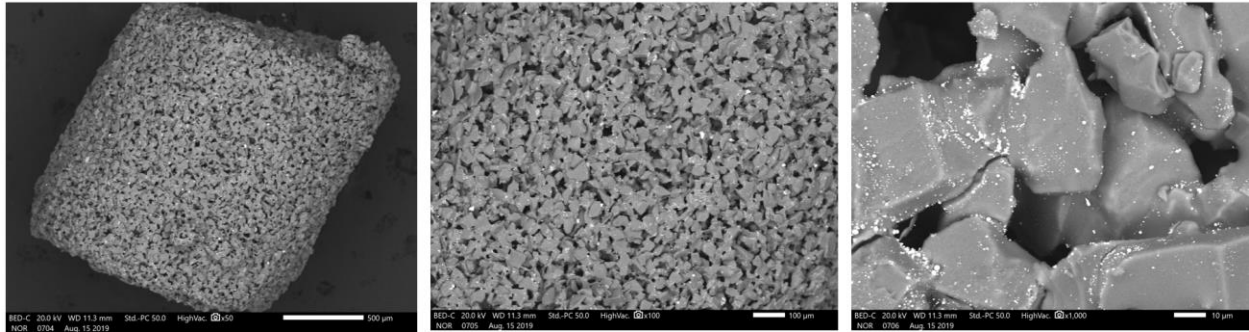


Figure 34: Scanning Electron Microscopy Analysis on Pellets near the Outlet Section

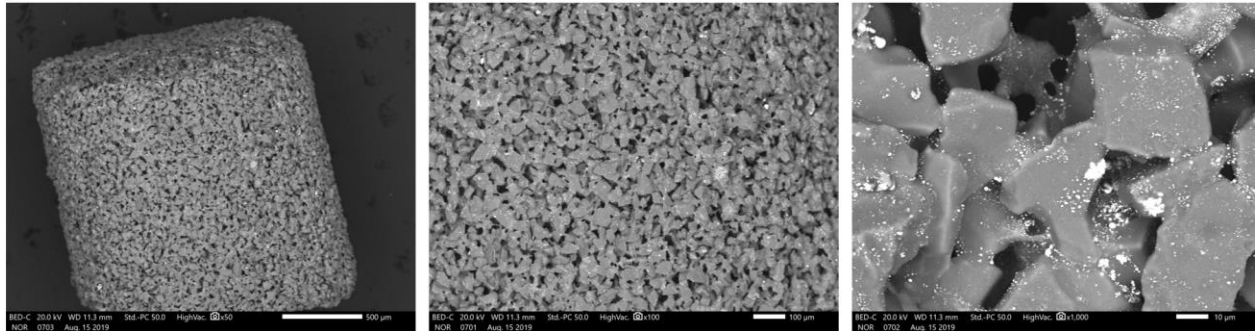


Figure 35: Scanning Electron Microscopy Analysis on Pellets near the Middle Section

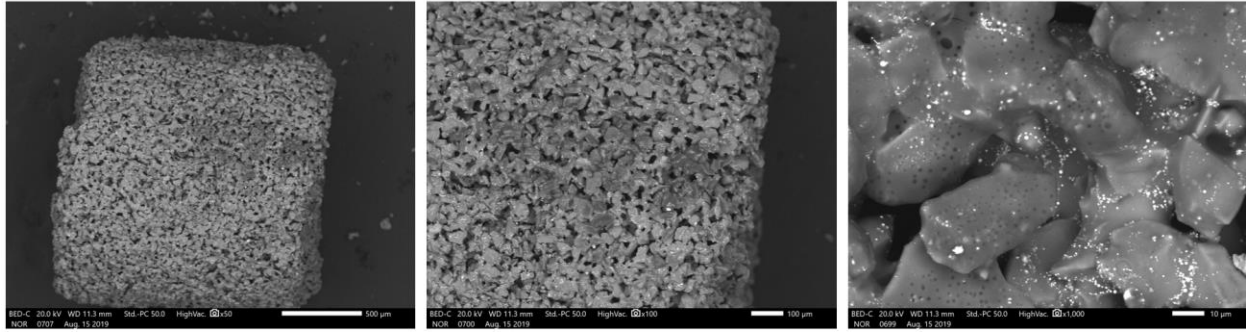


Figure 36: Scanning Electron Microscopy Analysis on Pellets near the Inlet Section

3.3.3 Energy Dispersive X-Ray Analysis on Silicon Carbide Catalyst Bed

Figure 37 below shows the energy dispersive x-ray analysis performed on a single silicon carbide pellet. This pellet was analyzed after the duty cycle test had been completed. From the graph, the several peaks represent the different elements or compounds detected by the x-rays. These different compounds are given in specific percentages present in table 4. 25.54% carbon and 54.79% was present from the ceramic itself, 17.49% from the catalytic material, and a small 2.18% possibly from the residual aluminum oxide left in the system from previous tests. The initial iridium loading factor for the silicon carbide pellets was 25%. Since the weight difference in the catalyst bed before and after the duty cycle testing is 0.658 g and the iridium loading factor difference is 7.51%, it is concluded that the silicon carbide catalyst bed lost catalytic material during the duty cycle tests. This is what explains the temperature peak rate of decay since essentially no silicon carbide pellet fractured.

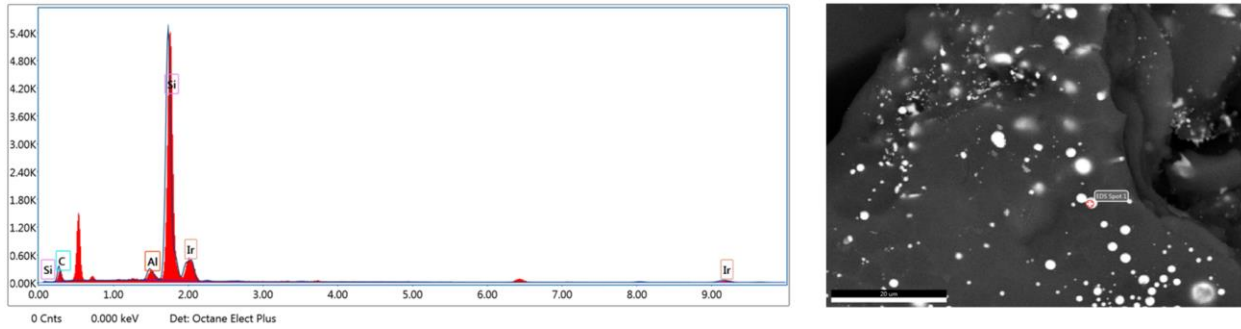


Figure 37: Materials Present on a Silicon Carbide Pellet

Table 4: Percentage of Materials Present on Silicon Carbide Pellet Post Duty Cycle Testing

Element	Weight %
C K	25.54
AlK	2.18
SiK	54.79
IrM	17.49

Chapter 4: Summary and Conclusion

4.1 Summary

Three different catalyst bed designs were produced to be integrated into a 1N AF-M315E thruster. The designs use three different ceramic substrates in the form of cylindrical pellets. The ceramic materials used are aluminum oxide, tungstated zirconia, and silicon carbide. The ceramic pellets were heat treated to reinforce their mechanical strength. A test setup was assembled to fully characterize these catalyst beds. Experiments were conducted to find the temperatures the decomposition of AF-M315E would produce with these catalyst beds. Duty cycle tests performed on each individual catalyst bed revealed their respective lifetime. In terms of these two parameters, the silicon carbide based catalyst bed had the highest performance.

4.2 Conclusion

All three of the catalyst beds produced AF-M315E decomposition temperatures of approximately 1400°C for mass flow rates in the range of 0.195 to 0.341 g/s. This was expected since the catalytic material was iridium with a similar loading factor for every case. 1400°C is enough temperature to create thrust and support propulsion in a monopropellant system. Therefore, these three catalyst bed designs can create the gas conditions desired in the combustion chamber for a 1N thruster.

Although all three catalyst bed designs are able to create the conditions to propulsion thrust in a 1N AF-M315E thruster, their lifetime, or how long they are able to produce high decomposition temperatures, varied significantly. At the lowest end of the lifetime performance scale was the tungstated zirconia pellets catalyst bed. These said pellets completely pulverized, rendering them useless, after only 22 duty cycle tests or 943 seconds. In powder form, the catalyst bed will quickly wash away through the nozzle with the incoming propellant. The next best

performing catalyst bed was the aluminum oxide based. These pellets were able to survive for 4203 seconds with approximately 22% of the catalyst bed fracturing. The highest performing catalyst bed was the silicon carbide based. The duty cycle for these pellets lasted for 3680 seconds and the catalyst suffered virtually no mechanical damage. The only anomaly found was a chunk of pellets bunched and bonded together presumably from the residual AF-M315E. With no fracturing of the silicon carbide catalyst bed, it is by far the superior choice for long duration missions that will require large total impulses. The silicon carbide catalyst bed also performed best in terms of the decomposition temperature peaks rate of decay which was only 2.56 °C/Test. With the smallest rate of decay, the highest lifetime, and the overall decomposition effectiveness of AF-M315E, silicon carbide based catalyst bed is the superior choice for propulsion applications.

It was observed that the peak decomposition temperatures produced with the silicon carbide catalyst still gradually decayed. With no fracturing of the pellets occurring to explain this decay, it was hypothesized that the iridium had washed away from all the incoming propellant. To test this theory, a series of scanning electron microscopy (SEM) and energy dispersive x-ray spectroscopy (EDS) were conducted on the post duty cycle pellets. The analysis showed that some catalytic material, or iridium, had been lost in the duty cycle experiments. Specifically, approximately 8% of the iridium had been lost. This is believed to be the cause of the gradual decay of the AF-M315E decomposition temperatures when the silicon carbide catalyst bed is used.

Chapter 5: Future Work

5.1 Lattice Pressure Drop Tests

The Center for Space Exploration and Technology Research received seven printed lattice cubes from NASA Marshall Space Flight Center. Three of the cubes are 10 mm³, and the other four are 12 mm³. These were printed out of titanium 64. These cubes were given to the OFX team to perform pressure drop tests across them. The experimental setup used for performing these pressure drop tests can be seen below in figure 38.



Figure 38: Lattice Pressure Drop Test Experimental Setup

The experimental schematic is shown in figure 39. From this schematic, it can be seen that the lattice cube sample sits between two pressure transducers that measure the pressure of the fluid before and after. The pressure drop is determined by taking the difference between PT-01 and PT-02. The pressurizing fluid is nitrogen and is regulated using a K-bottle regulator and a gas flow meter.

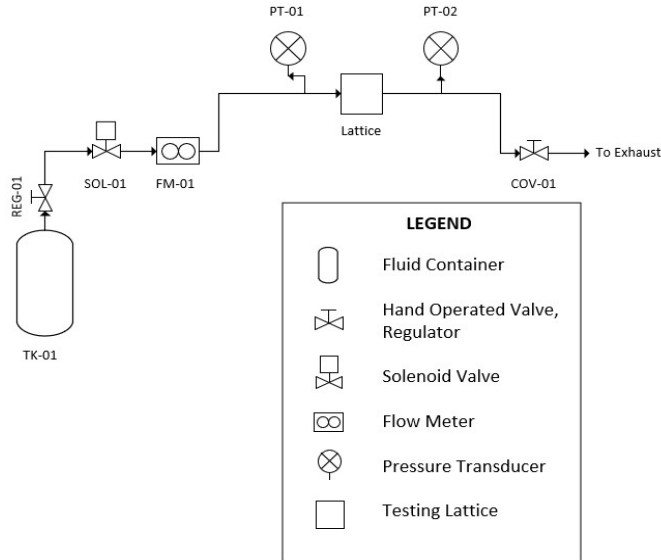


Figure 39: Lattice Pressure Drop Test Experimental Schematic

Currently, the team has tested one of the 10 mm³ lattice cubes codenamed “Pentagon”. The results for the pressure drop tests for Pentagon can be seen below in table 5. From the table, it can be seen that five different pressures were tested ranging from 20 psi to 100 psi. For all five of the tests, no mass change was detected for the lattice cube. Table 6 below the codenames and the respective cube sizes for the lattices that will continue to be tested in the near future.

Table Error! No text of specified style in document.: Lattice Cube Pressure Drop Test Results

Test #	Cube Size (mm ³)	Lattice Type	Orientation	Fluid	Tank Pressure (psi)	Mass Flow (g/s)	Initial Pressure (psi)	Final Pressure (psi)	Pressure Drop (psi)	Mass Change (g)
1	10	Pentacube	XZ	N2	20	0.79	12	6	6	0
2	10	Pentacube	XZ	N2	40	1.46	25	15	10	0
3	10	Pentacube	XZ	N2	60	2.13	40.2	24	16.2	0
4	10	Pentacube	XZ	N2	80	2.81	55.8	35	20.8	0
5	10	Pentacube	XZ	N2	100	3.49	69.8	45	24.8	0

Table 6: Lattice Cube Sizes and Names

Cube name	Cube size mm ²
Hexa	10
Grass hoper	10
Penta Cube	10
27	12
28	12
29	12
30	12

The purpose of these tests is to obtain a good understanding of the pressure losses these lattice designs will create. With the pellet catalyst beds mostly characterized, the Center for space Exploration and Technology Research is moving in the direction of producing its own printed catalyst design using additive manufacturing capabilities. These printed catalyst beds can be in the form of pellets or as a single monolithic ceramic foam that will be coated with catalytic material such as iridium.

References

- [1] Davoli, F., Kourogiorgas, C, Marchese, M., Panagopoulos, A., Patrone F. “Small satellites and CubeSats: Survey of structures, architectures, and protocols”. *Int J Satell Commun Network*. 2019;37:343–359. <https://doi.org/10.1002/sat.1277>
- [2] Tsay, M., Feng, C., Paritsky, L., Zwahlen, J., Lafko, D, Robin, M. “Complete EM System Development for Busek’s 1U CubeSat Green Propulsion Module.” 52nd AIAA/SAE/ASEE Joint Propulsion Conference, AIAA Propulsion and Energy Forum, July 25-27, 2016, Salt Lake City, UT.
- [3] Mueller, J., Hofer, R., Ziemer, John. “Survey of Propulsion Options for Cubesats.” 57th JANNAF Propulsion Meeting, Colorado Springs, CO, May 2010, paper 1425.
- [4] Tummala, A., R., Dutta, A., “An Overview of Cube-Satellite Propulsion Technologies and Trends” Department of Aerospace Engineering Wichita State University.
- [5] Masse, R., K., Allen, M., Driscoll, E., Spores, R., A., Arrington., L., A., Schneider., S., J., Vasek, T., E., “AF-M315E Propulsion System Advances and Improvements” 52nd AIAA/SAE/ASEE Joint Propulsion Conference, July 25-27, 2016, Salt Lake City, UT
- [6] Vazquez, A., “Design and Development of a Hydrogen Peroxide Monopropellant Thruster System” Thesis, Department of Mechanical Engineering at the University of Texas at El Paso, 2015.
- [7] Barragan, J., “Development of an ADN Based Ionic Liquid Monopropellant Modular Test Bed” Thesis, Department of Mechanical Engineering at the University of Texas at El Paso, 2015.
- [8] Tsay, M., Chelmsford, N., Hruby, V., Grenier, C., Costao, W, Lafko, D. “Long Life Thruster.” Patent Application Publication. US 2015/0001346 A1 Busek Co. January 1, 2015.
- [9] Polaha, J. “Internal Resistive Heating of Catalyst Bed for Monopropellant Catalyst” Patent Application Publication No: US 2011/0165030 A1, Aerojet Rocketdyne Co. July 7, 2011
- [10] Vazquez, A., Aguilar, D., Mejia, J., Cuevas, R. “Development of An Iridium Catalyst for The Decomposition of Green Monopropellants.” University of Texas at El Paso, Joint Army NASA Navy Air Force Conference and Exhibit 2018
- [11] Mejia, J., Vazquez, A., Cuevas, R. “Development of an Iridium Catalyst for The Decomposition of Green Monopropellants and Testing of 1N Thruster.” University of Texas at El Paso, Joint Army NASA Navy Air Force Conference and Exhibit 2019
- [12] Vazquez, A., Cuevas, R., Mejia, J., Valenzuela J. “Development of an Aluminum Oxide, Zirconia, and Silicon Carbide based Iridium Catalyst for the Decomposition of AF-M315E.” University of Texas at El Paso, Joint Propulsion Conference and Exhibit, 2019
- [13] Valenzuela J, Mejia, J., Vazquez, A., Cuevas, R. “Development and Testing of a 1N AF-M315E Thruster for Small Satellite Applications.” University of Texas at El Paso, Joint Propulsion Conference and Exhibit, 2019

Vita

Alejandro Vazquez was born in El Paso Texas, on September 5 1990. He attended and completed his high school education at America's High School in El Paso Texas in 2009. That same year he enrolled at the University of Texas at El Paso and graduated in 2013 with a bachelor's of science in mechanical engineering. During his undergraduate studies, Alejandro worked under the mentorship of Dr. Choudhuri at the Center for Space Exploration and Technology Research. He was part of the team developing the H₂O₂ micro thruster technology and also the team conducting the flame characteristics of the new novel monopropellant, LMP-103s. He continued his education by pursuing a master's of science in mechanical engineering at the University of Texas at El Paso. During the summer of 2015, Alejandro joined NASA's Kennedy Space Center's team as part of an internship program. During his time there, he worked on In Situ Resource Utilization projects involving the development of robotics for Mars exploration. Alejandro decided to pursue his doctorate degree and enrolled in the mechanical engineering PhD program at UTEP in summer 2016. Most of his PhD work involve the investigation of ionic green monopropellants.

Contact Information: aavazquez2@miners.utep.edu